UNIVERSITY OF TURKU

Effects of corticosterone-induced depression in mouse default mode network

Institute of Biomedicine
MDP in Biomedical Sciences, Drug Discovery and Development
Master's thesis

Author:
Tommi Kiiso

Supervisors:
Professor Eero Castrén
MSc Raz Balin
Professor Ullamari Pesonen

13.05.2025
Turku

Master's thesis

Subject: Institute of Biomedicine, MDP in Biomedical Sciences, Drug Discovery and Development
Author: Tommi Kiiso
Title: Effects of corticosterone-induced depression in mouse default mode network
Supervisor(s): Prof. Eero Castrén, MSc Raz Balin, Prof. Ullamari Pesonen
Number of pages: 56 pages
Date: 13.05.2025

Major depressive disorder (MDD) is a major cause of disability globally, with approximately 300 million people suffering from it worldwide. Current antidepressant treatments rely heavily on selective serotonin reuptake inhibitors, as well as selective noradrenaline reuptake inhibitors, and tricyclic antidepressants. However, these drugs are associated with long onset times, which can be preceded by serious adverse effects such as changes in weight, increased anxiety, and sexual dysfunction, and roughly 30 % don't respond to current antidepressants properly. Additionally, the development of novel antidepressants has not achieved any major breakthroughs in several decades, meaning there remains a large unmet medical need in the treatment of depression. The default mode network (DMN) is one of the major resting-state networks, that has been characterised to have increased activity during internally oriented tasks, such as self-referential thinking, and decreased activity during externally oriented tasks, such as focused studying. The DMN has been previously shown to have altered activity in MDD patients, and it has been hypothesised that the increased activity of the DMN would be related to certain symptoms of MDD, like rumination and negative self-image. Therefore, researching the DMN's functionality in healthy mice and mice with depression-like characteristics could provide new insights on its role in depression and possibly aid in the development of novel antidepressants.

The aims of this thesis were to model the DMN in a depression-like state in mice to gain more knowledge of the DMN's functional connectivity and activity in mice, and to study the oscillatory synchrony dynamics within the DMN to learn about its pathological characteristics in depression. By utilizing a novel electrophysiology setup consisting of two intracranial Neuropixels probes, and two cortical micro-electrocorticography grids, we recorded the activity of the DMN in healthy, control mice, and in mice that were administered corticosterone via drinking water for 21 days to model depression.

In this study, we observed a decrease between the baseline and post-treatment synchrony in the posterior DMN regions and increase in the anterior DMN regions within the treatment group. Also, a dissociation between the front and back regions of the DMN was observed in the treatment group. With the functional connectivity, there was a clear decrease in the posterior sections and a more subtle increase in the anterior sections. Furthermore, no alterations in synchrony or connectivity were not observed in the control group to the same extent, suggesting a difference between the groups.

In conclusion, depression-like state seems to alter the synchrony and functional connectivity of the DMN, possibly relating to symptoms of MDD, such as rumination and impaired memory control. However, due to a very small sample size and a topic with high variability in results, no clear conclusions could be made based on these results. Therefore, future studies need to confirm the results with larger cohorts, and comparison to equivalent human data acquired by EEG/MEG could provide translational value and more insights on the functionality of the mouse DMN.

Keywords: Depression, Default Mode Network, Electrophysiology, Neural plasticity

Table of contents

1 Introduction

Major depressive disorder (MDD), also known as clinical depression, is a major cause of disability globally. It is estimated that approximately 300 million people worldwide suffer from MDD with the prevalence increasing yearly (Cui et al., 2024). As MDD is a heterogenous disease, its symptoms can vary from case to case but the fundamental symptoms of MDD include depressed mood and anhedonia. Additionally, symptoms may include emotional symptoms such as suicidal thoughts, neurocognitive symptoms such as decreased ability to think or concentrate, and neurovegetative symptoms such as changes in appetite or weight (Malhi & Mann, 2018).

The pathophysiological factors and aetiology of MDD are not completely clear but it is commonly accepted that MDD develops due to multiple factors. Popular hypotheses that are closely associated with MDD pathogenesis, include the dysfunction of the hypothalamus-pituitary-adrenal (HPA) axis, abnormal monoamine and cytokine levels, and multiple genetic factors. Additionally, environmental factors, such as traumatic or stressful life events can have a major role, especially in the onset of depression (Cui et al., 2024).

Excluding psychotherapy, current first-line treatment options for MDD include selective serotonin reuptake inhibitors (SSRIs) such as fluoxetine or escitalopram. Alternative common pharmacological treatment options include serotonin and noradrenaline reuptake inhibitors (SNRI) and tricyclic antidepressants, but also monoamine oxidase inhibitor moclobemide to some extent. However, approximately 30 % of MDD patients don’t respond to current treatments effectively, creating a large unmet medical need in treating depression. Additionally, current drug treatments can take multiple weeks to show reduction in depressive symptoms and severe adverse effects may precede the improvement (Hillhouse & Porter, 2015). Therefore, development of novel, more effective, and fast-acting antidepressants is needed.

In the brain, MDD has been shown to alter the structure as well as the functional connectivity of different brain regions. Commonly, imaging studies have demonstrated decreased volume within the prefrontal cortex (PFC) and hippocampus as well as abnormal activity of the major resting-state networks which are the default mode network (DMN), the salience network (SN), and the central executive network (CEN). They represent the brain’s function during rest, cognition, and emotional processes. More thoroughly, the activity of the DMN seems to be increased while the activity of SN and CEN is decreased in MDD patients. (Duman et al., 2019).

By investigating the DMN with electrophysiological methods in healthy and depressed states, new insights can be gained from its function that ultimately can help in the development of new antidepressant drugs with novel mechanisms of action.

1.1 Default mode network

The default mode network (DMN) was first identified in a meta-analysis conducted by Shulman et. al. in 1997 which described a neural network that is consistently suppressed during externally oriented tasks (Shulman et al., 1997). Later, when describing this resting-state neural network, the name default mode network was established (Raichle et al., 2001). Although the first DMN discoveries were made accidentally by observing suppressed brain regions in response to external tasks, it was soon realised that the DMN also plays an important role in cognition. Furthermore, following the emergence of the DMN as its own research area around two decades ago, these functional roles of the DMN have become clearer. Overall, the DMN's function is associated with internally oriented tasks that involve e.g. thinking about oneself, envisioning past or future events, and creating scenes in imagination. In addition to self-referential thoughts, the DMN also has roles in social cognition where it is active during certain social cognitive tasks such as moral judgement and understanding social cues (Smallwood et al., 2021). So, although the DMN was first thought to be active only when the brain is in so-called default mode which would include tasks like daydreaming and other spontaneous thought processes, it has later been shown to have an important role in higher-order cognition.

Anatomically, the DMN consists of multiple different brain regions, and it has been proposed that instead of one large network it would consist of two or more separate juxtaposed subnetworks that are connected along the midline. This is supported by studies investigating tasks that are known to activate the DMN but differ slightly, such as judgement about people versus places. Both these tasks activate regions within the DMN, but different types of tasks activate regions that are spatially separated which implies that there would be highly specialized subnetwork within the canonical DMN (Buckner & DiNicola, 2019). The core regions associated with the canonical DMN and shown in figure 1 include the ventral and dorsal medial prefrontal cortex (vMPFC/dMPFC), posterior cingulate cortex (PCC), retrosplenial cortex (Rsp), inferior parietal lobule, and the hippocampal formation. In addition to these regions there are several other areas that are shown to be active during tasks associated to DMN function as well as functionally connected to each other (Buckner et al., 2008).

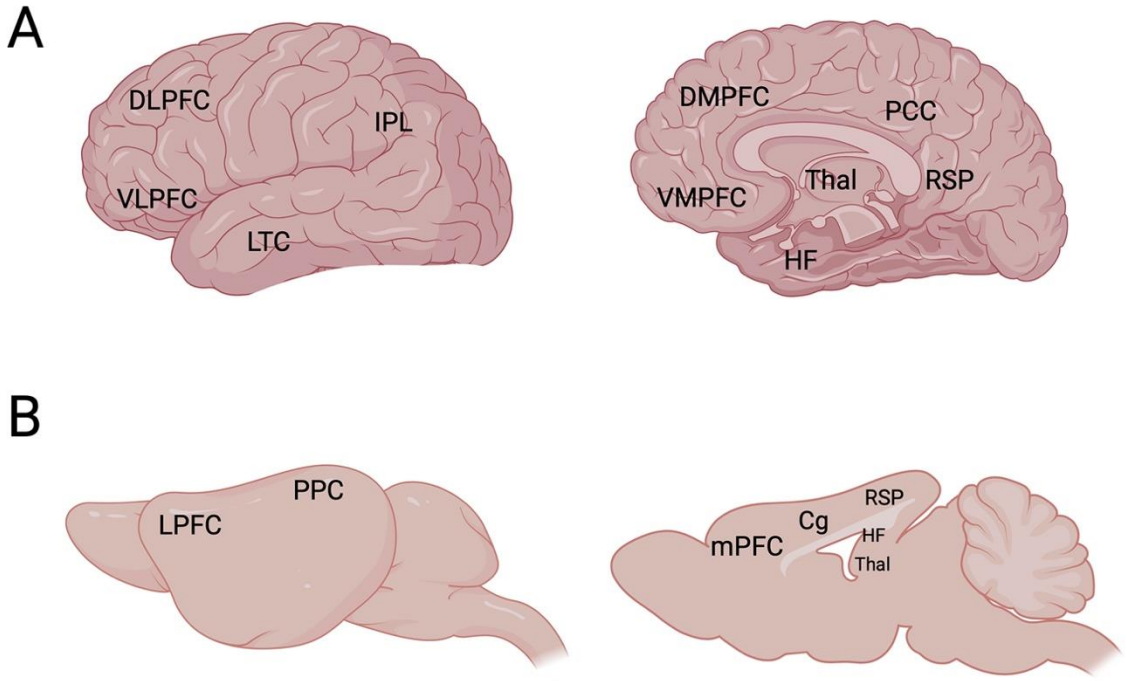

Figure 1. Homologous DMN-relevant regions of human (A) and mouse (B) brain in lateral and sagittal views. Lateral views are presented on the left and midline sagittal cuts are presented on the right. DMN-associated regions in humans include the dorsolateral prefrontal cortex (DLPFC), ventrolateral prefrontal cortex (VLPFC), lateral temporal cortex (LTC), inferior parietal lobule (IPL), dorsomedial prefrontal cortex (DMPFC), ventromedial prefrontal cortex (VMPFC), thalamus (Thal), hippocampal formation (HF), posterior cingulate cortex (PCC), and retrosplenial cortex (RSP). In mice the DMN associated regions include lateral prefrontal cortex (LPFC), posterior parietal cortex (PPC), medial prefrontal cortex (mPFC), cingulate cortex (Cg), RSP, HF, and thalamus. Human DMN areas are based on (Buckner et al., 2008) and mouse DMN areas are based on (Whitesell et al., 2021). Created in BioRender.

1.1.1 Default mode network in depression

The DMN has been shown to have altered function in several psychiatric disorders such as autism and schizophrenia but also in depression. In MDD patients, the connectivity within the DMN regions has increased and the overall ability to deactivate the DMN has decreased, leading to hyperactivity of the DMN (Kaiser et al., 2015). Increased activity can be seen especially in subgenual-cingulate cortex, the thalamus, the orbitofrontal cortex, and the precuneus areas, all of which are subregions of the previously described DMN core regions. Additionally, within the DMN, MDD patients show altered connectivity between the anterior and posterior subnetworks. However, studies have reported both, dissociation and increased connectivity, between these regions, making findings inconsistent (Mulders et al., 2015).

Overall, these changes can possibly lead to more self-involved and ruminative thinking patterns, which are common symptoms in depression (Marchetti et al., 2012).

On a network level, the connectivity between the DMN and the frontoparietal network, another resting state network involved in regulation of attention and emotion, shows to be increased, possibly enhancing the symptoms associated with DMN's increased activity. When comparing the connectivity of the DMN to the two other major resting-state networks, SN and CEN, the posterior regions of DMN have decreased connectivity to both SN and CEN while the anterior DMN regions have increased connectivity with the SN (Mulders et al., 2015).

Overall, previous studies in MDD patients have consistently shown hyperactivity in the DMN which is associated with ruminative self-referential thoughts likely leading to maladaptive changes. Additionally, the DMN's connectivity to other resting-state networks is altered in MDD patients with decoupling of the DMN from the two other major resting-state networks being a common finding. This can lead to impaired transitioning from one network to another and dysfunctional network activity.

1.1.2 Translationality between human and mouse DMN

Originally, the DMN was identified in humans and majority of the research on the DMN focuses on humans. However, as this research is conducted in mice, it is important to acknowledge the anatomical and functional differences between human and mouse DMNs and the overall translational value of the research. A review by Gozzi and Schwarz discusses studies focusing on the DMN in rodents and shows that an analogue DMN consisting of comparable brain regions can be found in mouse and rat brains (Gozzi & Schwarz, 2016). However, as the review highlights, not all studies have identified a DMN-like network in rodents which is possibly due to differences in study protocols such as anaesthesia depth. Regardless of these controversies, several different publications have demonstrated reliable DMN analogues in rodents suggesting that there is conserved DMN regions between species (Gozzi & Schwarz, 2016).

As mentioned, mice do have DMN analogues but when compared to humans, some regions of this network differ slightly. Brain regions identified in mice include the orbitofrontal cortex, cingulate cortex, and parietal cortex as well as primary visual area and somatosensory area. These regions align with previous studies on rat DMN suggesting that the DMN is similar between rats and mice but when compared to humans the differences are more notable (Stafford et al., 2014). Compared to humans the murine DMN does not include as large PFC areas

especially in the infralimbic and prelimbic cortices of the PFC. Additionally, the connectivity between the anterior and posterior sections involves the entire midline in the murine DMN whereas in humans the connectivity is more precise between specific regions. Functionally, the murine DMN seems to have similar roles as the human DMN of processing information during idle states, just with less higher order cognitive functions (Lu et al., 2012). Additionally chronic stress, a common factor in depression, has been shown to increase the functional connectivity within the rat DMN similarly to humans with MDD suggesting that the murine DMN has similar features in pathological conditions as humans (Henckens et al., 2015).

In conclusion, although mouse and human DMNs have certain differences in both anatomy and connectivity, research on DMN conducted in mice have translational value also in humans as the functionality is similar in both species. However, examining between species DMN homology should be interpreted with care as linking corresponding regions can be difficult. All in all, the mouse DMN works as a decent model to study alterations in the network which helps to better understand the DMN's function in healthy and pathological states (Stafford et al., 2014).

1.2 Brain criticality and plasticity

In order to observe and measure brain's activity it is important to understand how it functions. In understanding brain activity, research on specific neural mechanisms have played an important role in unveiling questions regarding brain function, but on a larger scale it is harder to explain how the brain comes together to function as a single organ with numerous important roles. In the past decades, neuroscientists have proposed that brain network dynamics operate according to a general theory of natural systems called the criticality theory, which would partly explain the relationships between neural mechanisms and cognitive functions. According to the theory, dynamic systems that can go through phase transitions, such as brain transitioning between excitative and inhibitive states, can operate near a point between the phases where small changes in the system could lead to increased inhibition or excitation. Ultimately, the benefits of operating at this critical zone would include optimal transfer, processing, and storage of information in the brain as well as increased adaptability to environmental stimuli (Cocchi et al., 2017).

When a system operates in the critical zone without external tuning of the system such as in the brain, it is referred to as self-organized criticality. In these self-organized systems, the criticality is achieved by the systems own tuning that makes it possible to remain in the critical region. In

brain, the self-organization is supported by the network connectivity, synaptic strength, excitation/inhibition-balance, and most importantly, neural plasticity which controls all the previous factors (Heiney et al., 2021). Through neural plasticity, external and internal factors become represented in an individual's neural structure where simply put, active connections are strengthened and inactive are weakened or eliminated. However, without control these connections following the so called Hebbian plasticity mechanisms, would grow uncontrollably resulting in positive feedback loops and unfavourable network dynamics. Therefore, homeostatic plasticity acts as counterbalancing factor through negative feedback loops by decreasing connectivity in response to high neuronal activity and increasing it in response to low neuronal activity (von Bernhardi et al., 2017). Altogether, in relation to the brain criticality theory, mechanisms of plasticity would enable self-organization into the critical zone where optimal brain operating capabilities would be achieved (Heiney et al., 2021).

1.2.1 Neural oscillations

Neural oscillations, or rhythms in neural activity originate from synchronized electrical signals generated by neuron populations that can be observed directly with invasive recording methods or indirectly with for example the EEG. These brain oscillations act as a basis for neuronal processing in larger neural networks, where they can be used to study brain dynamics within the network (Thut et al., 2012). Based on their frequencies, the oscillations are often divided into delta, theta, alpha, beta, and gamma bands with each band having certain cognitive functions linked to them listed in table 1 (Herrmann et al., 2016).

Table 1. Characterization of different human brain oscillations. Based on (Herrmann et al., 2016).

Name	Frequency (Hz)	General cognitive functions
Delta	0.5 – 4	Sleep
Theta	4 – 8	Deeply relaxed with inward focus, inhibitive functions
Alpha	8 – 12	Relaxed with passive attention
Beta	12 – 35	Normal wakeful consciousness and concentration
Gamma (High Gamma)	35 – 90 (50 <)	Active information processing, deep concentration

In relation to depression, especially alpha and theta oscillations have been reported to have altered activity in MDD patients. Both frequencies are widely studied in depression. With alpha

waves, a common finding among MDD patients is cortical frontal alpha asymmetry (FAA), where the activity of alpha waves is greater on the left side. This asymmetry is linked to abnormalities in reward processing and managing of positive emotions which would relate to common MDD symptoms such as anhedonia. However, studies regarding the FAA are contradicting with several studies failing to see differences between control group and MDD patients making it an unreliable marker of depression (Fernández-Palleiro et al., 2020). Aside from the FAA, the connectivity of alpha waves is commonly increased within the DMN's anterior and midline areas whereas in the posterior regions alpha activity has been more reduced (Ippolito et al., 2022).

Theta activity is another frequency that is previously observed to be altered in MDD patients, although the direction of alteration varies among studies between increasing and decreasing activity (Fernández-Palleiro et al., 2020). Within the DMN, theta rhythms are most prominent in the hippocampal formation and in the frontal midline of the PFC, more specifically in the ACC. These regions are relevant for memory and attention processing as well as cognitive processing, which all are linked to symptoms in MDD (Wang, 2010). Among MDD patients, an increase in the theta activity in subgenual ACC is a common finding, although decreases have also been reported (Fernández-Palleiro et al., 2020). Hippocampal theta activity on the other hand seems to be more commonly decreased in depressed individuals (Kane et al., 2019). Altogether, the inconsistencies between results in alpha and theta activities suggests that the abnormalities are more dependent on individual variability and the subtype of depression rather than other factors such as methodological differences.

In addition to frequency, electrophysiological signal's amplitude and phase play an important role in oscillatory synchrony dynamics. Amplitude refers to the strength of the signal in which higher amplitude associates with more synchronous neuronal firing. Phase on the other hand describes the position of the oscillatory cycle at a certain time point which is relevant for temporal synchrony between brain regions. In other words, if two signals had the same frequency and amplitude but different phase, their coordination would be less effective (Hahn et al., 2019). Altogether, frequency, phase, and amplitude are main parameters at play when looking at oscillatory synchrony dynamics. Neuronal oscillations and changes in the synchrony between areas most likely affect the behavior which is why they are of great interest when researching brain disorders (Thut et al., 2012).

The synchrony of the oscillation frequencies over time, as well as the synchrony between different brain regions can reveal fundamental information about brain dynamics' relation to cognitive functions and behaviour. Commonly, the level of synchrony seems to be moderate among healthy people meaning that the overall sum of excitation and inhibition remains neutral or near the critical point. However, the mean synchrony levels vary significantly between healthy individuals which can be associated with the differences in cognitive functions between individuals. Therefore, it has been proposed that instead of a single critical point the brain would operate in an extended region of criticality called the Griffiths phase which would address the variability in brain dynamics between individuals. Furthermore, the oscillatory synchrony dynamics become abnormal in many brain disorders and start to manifest either excessive or inadequate network synchrony dynamics also known as supercriticality or subcriticality, respectively (Fuscà et al., 2023).

1.2.2 Brain criticality

As described before, according to the brain criticality theory, the brain operates at a region between subcriticality and supercriticality where the handling of information would theoretically be optimal. Additionally, this would improve the adaptability to environmental stimuli, as in the critical region transitioning between excitatory and inhibitory activity would require only a small stimulus to create critical neuronal avalanches which are bursts of activity that follow power-law distribution between avalanche probability and avalanche size. This means that in the critical zone avalanche sizes do not have a predominant size but are diverse and scale-free. Also, brain functioning in the critical region would enable activity to return to baseline after the stimuli is gone and not continue in the supercritical or subcritical regions. Studies regarding criticality have however noticed that typical characteristics of criticality get suppressed during task performance meaning that the criticality theory would be more applicable to resting-state networks. This is partly explained by a need to be able to react to unexpected sensory inputs in resting-state but also criticality would allow the brain to explore a broad range of mental states during resting periods which would prepare the brain better for different situations (Cocchi et al., 2017).

When looking at the role of criticality on a brain network level, it is suggested that operating at the Griffiths phase brings a dynamic stability where switching activity between different networks as well as the cooperation between networks is functional. This means that within the networks the synchrony of oscillations is moderate. As depicted in figure 2, if brains functioned

deeply in the subcritical zone, different brain regions wouldn't be functionally coupled resulting in uncoordinated activity and inadequate responses to stimuli. On the other hand, if brains functioned in the supercritical zone, different regions would be coupled too closely resulting in unspecific network activity where single stimulus could activate multiple networks. Therefore, Griffiths phase enables the networks to exhibit neuronal avalanche dynamics that extends the number of adaptive responses the network can produce to maximum (Palva & Palva, 2018). However, even though it would be computationally optimal to stay in the critical zone, it is suggested that the brain operates slightly in the subcritical regime possibly creating a buffer against the supercritical zone while still preserving similar features as in the critical zone. Additionally, not all tasks such as focused attention are optimized at criticality and operating at slightly subcritical zone, the activity could be more controlled than in the critical zone (O'Byrne & Jerbi, 2022).

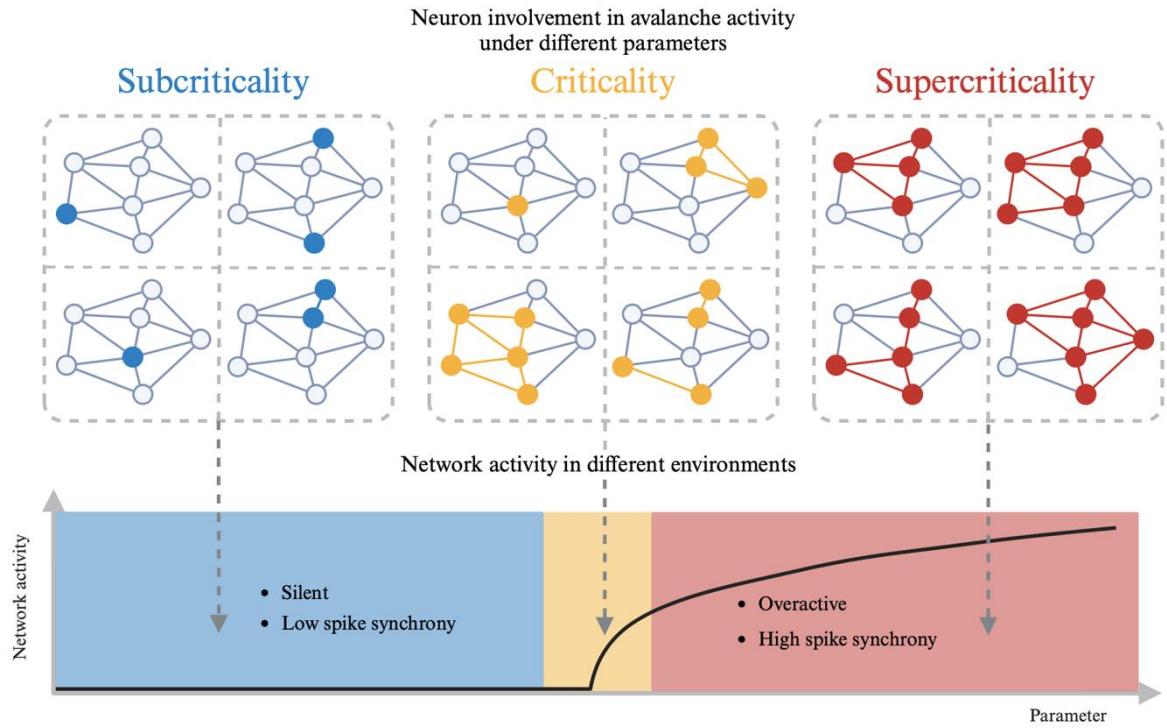

Figure 2. Role of criticality in neural avalanches and network activity. The upper section describes a generalization on how neuronal avalanches form under different criticality states in four different random situations. The lower section describes how these avalanches correspond to overall network activity in different environments (parameters) inside resting state brain networks. In the subcritical regime the overall activity and synchrony across networks is low while it is the opposite in the supercritical regime. In the critical zone these properties even out and neuronal avalanches become diverse in size promoting broader range of computational capabilities in the brain. Created in BioRender.

From a disease point of view, criticality can also help to describe abnormal network synchronization dynamics. In many neurological diseases the synchrony dynamics are thought to deviate from the Griffiths phase into sub- or supercritical regions and not being able to

recover back to the critical zone of healthy brain. This has also been described in MDD, where the oscillatory synchrony dynamics within the DMN seem to shift towards supercriticality manifested with increased activity in some DMN regions, although results on this topic have been contradictive (Yan et al., 2019; Zhu et al., 2017). However, when looking more broadly at the brain function in MDD, the reduced neural complexity and flexibility linked to MDD would suggest that deeper subcriticality is dominant in depressed individuals and supercriticality would be observable only at certain subregions like the DMN (Zimmern, 2020).

Even though the brain criticality theory proposes a way to better understand brain functioning, it is good to remember that it is a theory and should be treated with consideration. The brain criticality theory remains widely debated and criticism towards the theory mainly addresses signature characteristics of criticality and how they can also be found in non-critical systems. Additionally, opposing opinions have pointed out the lack of similar experimental environments between studies regarding brain criticality as well as defects in statistical testing methods (Destexhe & Touboul, 2021). In turn, the criticism has been responded with developing new ways of assessing criticality in neural systems. However, the brain criticality theory remains as an open question and more work is required to address the questions regarding its role in brain functionality (Beggs, 2022). All in all, criticality remains as an interesting way of presenting activity and functional capabilities of the brain, and it can be used to some extent as a tool to explain abnormal neural activity during pathological states.

1.2.3 Neuronal plasticity

Neuronal plasticity enables the brain to change and adjust itself according to the environment. It is an essential mechanism that allows learning, memory, and overall brain functioning via trophic and atrophic neural processes (Power & Schlaggar, 2017). Neuronal plasticity is modulated by Hebbian plasticity that either increases or decreases the strength of synapses and by homeostatic plasticity that counterbalance the effects of Hebbian plasticity. In other words, Hebbian plasticity affects the transmission efficacy whereas homeostatic plasticity modifies more structural changes as a result of persisting neuronal activity (von Bernhardi et al., 2017). However, these plastic changes do not happen by themselves, but they need molecular mediators to enable the plasticity to happen in response to neuronal activity (Castrén & Antila, 2017).

Neurotrophic factors are a key group of molecules proposed to promote plasticity. Out of neurotrophic factors, the neurotrophin family and especially the brain derived neurotrophic

factor (BDNF) are interesting molecules from drug developmental point of view due to BDNF's abundant expression in the brain and their overall ability to promote neuronal plasticity. Other members of the neurotrophin family include nerve growth factor (NGF), neurotrophin-3 (NT-3), and neurotrophin-4 (NT-4). The neurotrophins bind to receptors from the Trk-family with NGF binding to TrkA, BDNF and NT-4 binding to TrkB, and NT-3 binding to TrkC. Additionally, all neurotrophins bind also to the p75 neurotrophin receptor. However, studies suggest, that the plasticity promoting effects are mediated trough binding of mature forms of neurotrophins to the Trk-family members whereas binding to p75 neurotrophin receptor mediates more atrophic neuronal events (Castrén & Antila, 2017).

As mentioned, BDNF is one of the most studied neurotrophin and its plastic effects have been tried to be replicated when developing novel therapeutics despite it is known that some already approved drugs, especially antidepressants, promote the production of BDNF or activate its receptor, TrkB, in other ways. However, these effects are mediated only after chronic antidepressant treatment whereas acute treatment does not have effects on BDNF expression (Castrén & Antila, 2017). The advantages of promoting plasticity through pharmacological compounds would be to achieve juvenile-like plasticity which is present in the critical periods early in life. In these critical periods the neuronal plasticity is heightened which allows more efficient tuning of neural networks ultimately making neural development much more flexible in young individuals (Hübener & Bonhoeffer, 2014).

Previously it was thought that after these critical periods the capacity for plasticity declines and remains relatively low throughout the rest of the life. However, recent studies have shown that critical period-like plasticity can be induced also in adults with certain pharmacological compounds. Among these compounds, antidepressants and more interestingly, psychedelics, induce critical period-like plasticity through binding to TrkB and allosterically regulating BDNF's potency and its levels in the brain (Casarotto et al., 2021; Moliner et al., 2023). Therefore, even in adults, neuronal networks that have pathological characteristics such as in depression, can be more easily rewired with the help of plasticity inducing compounds (Castrén & Antila, 2017).

As the plastic effects of conventional antidepressants are mediated only after chronic use and their affinity to TrkB is relatively low, it is thought that improving these shortcomings could be a goal for future antidepressant development. Therefore, psychedelics that bind to TrkB with higher affinity already after single dose have become a promising model for development of

novel antidepressants. However, treatment with psychedelics pose an issue due to their hallucinogenic effects which prevents their broad clinical use. This could still be overcome as it is suggested that the plasticity promoting effects and hallucinogenic effects are separately mediated via TrkB and 5HT-$_{2A}$ receptors, respectively. Therefore, it would be theoretically possible to develop compounds that possesses the rapid antidepressant and plasticity promoting effects without the hallucinogenic effects (Moliner et al., 2023).

All in all, neuronal plasticity results in a representation of an individual's environment. It is good to notice that plasticity cannot be positive or negative, but it is dependent on how the individual experiences their environment and only the results of plasticity are advantageous or maladaptive. Therefore, when using plasticity increasing drugs to treat psychiatric diseases it would be important to additionally have psychotherapy as an adjunct treatment to guide the plasticity for beneficial effects.

1.3 *In vivo* electrophysiology

For a long time, it has been known that the function of nervous system is closely linked to electrical activity. Since this discovery, the methodology to record the activity of neurons has advanced in giant leaps allowing research of the neural activity in multiple techniques. Furthermore, the advances in electrophysiological methodology have enabled better understanding of the activity in the nervous system, which is in the centre of several pathological conditions, making electrophysiology an important research tool in many topics (Cavanagh, 2019).

Over the last decades, *in vivo* methods have improved alongside other electrophysiological methods and recording equipment have progressively increased in number of recording sites per probe. More recently, intracortical technologies such as the Neuropixels, a silicon electrode probe, have increased the number of recording sites close to 1000 allowing larger and more precise recordings than before (Cavanagh, 2019). Additionally, surface level cortical recording technologies have developed from electrocorticography (ECoG) to micro-electrocorticography (µECoG) enabling better spatial resolution and suitability also for smaller animal models. Together, intracortical electrodes and µECoG provide more accurate signal with smaller noise-to-signal ratio when compared to EEG due to the electrodes being in direct contact with region of interest (Shokoueinejad et al., 2019).

Neuropixels probes were developed by Jun et al. in 2017 with the primary goals to have dense and extensive recording sites with small cross-sectional area to minimize damage to brain tissue (Jun et al., 2017). Although these improvements to previous extracellular probes create opportunities for electrophysiology recordings, Neuropixels probes also pose some challenges especially regarding the data processing. The data sets produced by Neuropixels are enormous as each probe creates approximately 1 GB of data per minute, meaning that a 30-minute recording with two separate probes creates around 60 GB of data solely from the Neuropixels probes. Therefore, in addition to issues with data storage that the data acquisition rate creates, the processing of the data is an even greater challenge (Steinmetz et al., 2018). However, in recent years the processing of the data has become much more automated and for example the spike sorting which has been a major issue with data processing can nowadays be fully automated (Mohammadi et al., 2024). Despite of these challenges, Neuropixels provide opportunities to study brain activity in novel ways and from broader regions than with previous technology. Overall, this can be utilized to study for example functional networks and how their activity relates to behaviour and disease (Steinmetz et al., 2018).

Another recording technique utilized in this thesis is the µECoG. ECoG electrodes are placed on the cortex where they can record local field potentials from cortical areas with high spatial resolution. The development of µECoG has provided even better spatial and temporal resolution due to smaller size and increased number of electrode sites. Additionally, the smaller size makes µECoGs more suitable for small animal models (Shokoueinejad et al., 2019). In combination with the intracranial probes the µECoG grids can provide electrophysiological information on entire functional networks, such as the default mode network. This is crucial for understanding how different regions of networks function together during health and pathological states (Lee et al., 2022).

Altogether, when using recording devices that are in direct contact with the regions of interest, the acquired data is spatially and temporally much more accurate with the signal-to-noise ratio also being higher. This provides advantages over human recordings in data accuracy although there is still work needed to confirm how different functional networks translate between species. The combination of ECoG system and Neuropixels system also allows to study the relationship between cortical regions and intracranial regions to see how they interact during healthy and pathological states. Overall, the recent advancements of *in vivo* electrophysiology provides methods to study brain functions in novel ways that can provide new insights on brain activity (Mercier et al., 2022).

1.4 Depression animal models

MDD is a complex and heterogenous disease that is a sum of certain environmental and genetic factors that can ultimately build up to the progression of the disease. Therefore, it has been difficult to model depression with animals and it is unlikely that a single animal model could depict all the characteristics of depression accurately. However, creating disease animal models is critical for developing novel therapeutics. Current depression animal models rely heavily on chronic exposure to stress via different methods, which has been shown to induce depression- and anxiety-like characteristics behaviourally, but also at the cellular and molecular level in the brain. Additionally, these models have shown responsiveness to antidepressant treatments adding validity to the models (Samuels et al., 2011).

Current common depression animal models include chronic mild stress (CMS), chronic social defeat, physical pain, and learned helplessness, which all induce stress through different methods in the animals (Song & Kim, 2021). Out of these, the CMS model is the oldest and most used method to induce depression-like characteristics in animals. However, it can be laborious and difficult to replicate accurately across different studies. Additionally, the CMS model can be complicated to perform if the animals have undergone intense operations such as a craniotomy surgery beforehand. Therefore, a pharmacological model, such as chronic glucocorticoid administration is a valid option to induce depression-like changes in animals (Samuels et al., 2011).

1.4.1 Corticosterone-induced depression model

As mentioned, current animal models rely on chronic stress to induce depression-like characteristics. This is due to increased stress, and the functioning of the HPA-axis, being closely associated with depression pathophysiology. Stress which activates the HPA-axis and therefore increases circulating glucocorticoid levels helps to reach maximal performing capabilities in acute situations. However, prolonged stress and constant elevated glucocorticoid levels can have harmful effects on the brain as well as multiple other organ systems. In the brain, elevated glucocorticoid levels have been linked to decrease the number of synapses and to cause atrophy in the PFC and hippocampus in rodent studies. Additionally, chronic stress seems to reduce the expression and function of BDNF, one of the main molecules mediating neuronal plasticity (Duman et al., 2016). Altogether, the effects of chronic stress on the brain morphology show how closely it is connected to depression.

In addition to increasing endogenous glucocorticoid production through chronic stress, depression-like characteristics seem to be possible to induce with chronic corticosterone administration as well. In this corticosterone-induced depression model, the behaviour as well as the brain morphology follow characteristics of depression similarly to other depression animal models (Murray et al., 2008). Furthermore, the effects of chronic corticosterone administration are reversible to some extent with antidepressant treatment, increasing the model's predictive validity as depression model, and providing ways to study effects of novel antidepressants (Planchez et al., 2019).

Even though the corticosterone-induced depression model induces behavioural and morphological changes in animals and therefore satisfies at least some aspects of construct validity and face validity, it still has certain flaws. Firstly, the model focuses only on the stress aspect of MDD whereas naturally occurring, depression has a complex aetiology. Also, the induction of depression lacks the environmental stress component which is one of the key factors in human MDD patients, possibly affecting the value of face validity. Lastly, variability in dosing protocols, especially when dosing via drinking water, needs to be considered when interpreting results (Planchez et al., 2019).

The aims of this thesis were to model the DMN in a depression-like state in mice and therefore gain more knowledge of the DMN's activity and functional connectivity between healthy controls and individuals with depression-like characteristics. Another aim was to study the oscillatory synchrony dynamics within the DMN to unveil its pathological characteristics in depression and to gain new insights of its function.

The hypotheses of this thesis were that EEG recordings conducted with µEcoG grids and Neuropixels probes would provide new information on the activity of the DMN in a depression-like state. The hypothesis included that abnormal excessive synchrony dynamics in the DMN are one of the driving factors of depression and therefore supercritical synchrony dynamics were expected. Additionally, it was expected that the DMN activity and functional connectivity would differ between treatment group and control group.

2 Results

This was a pilot study and therefore, the results consist of preliminary data with a very low sample size in both, control group (n = 3), and treatment group (n = 3). Due to this, reliable statistical testing could not be done within this study.

2.1 Neuropixels-probes

2.1.1 Phase locking value

Figures 3 and 4 show the phase locking value (PLV) synchrony heatmaps of the theta (4-8 Hz) (Figure 3) and alpha (8-12 Hz) (Figure 4) bands from the caudal Neuropixels electrode. Sections A and B represent the baseline values of the control group (n = 3) and treatment group (n = 3), respectively. Similarly, sections C and D show values from the second recording after the 21-day period, with C showing the control group and D showing the treatment group. The scalebar on the right shows that higher values, that indicate more synchronous connections, are depicted in warmer colours (red) and smaller values, indicating less synchrony between regions, are depicted in colder colours (blue).

In figures 3A and 3C showing the control group, there is a slight increase in the synchrony between the anteromedial visual area and the dentate gyrus and CA1 (0.5 to 0.7) suggesting changes in connectivity between the hippocampus and anteromedial visual area. Apart from this, the PLV synchrony remains relatively unchanged between the control group timepoints. In 3B and 3D, showing the treatment group, similar increase can be seen between the anteromedial visual area and hippocampus areas, although with lower baseline value (0.2 to 0.4). Additionally, the treatment group shows decreases in synchrony within the anteromedial visual area layers (0.8 to 0.5) but also slight decreases between the posterior complex of thalamus and dentate gyrus (0.9 to 0.7). No statistical significance could be shown due to small sample size.

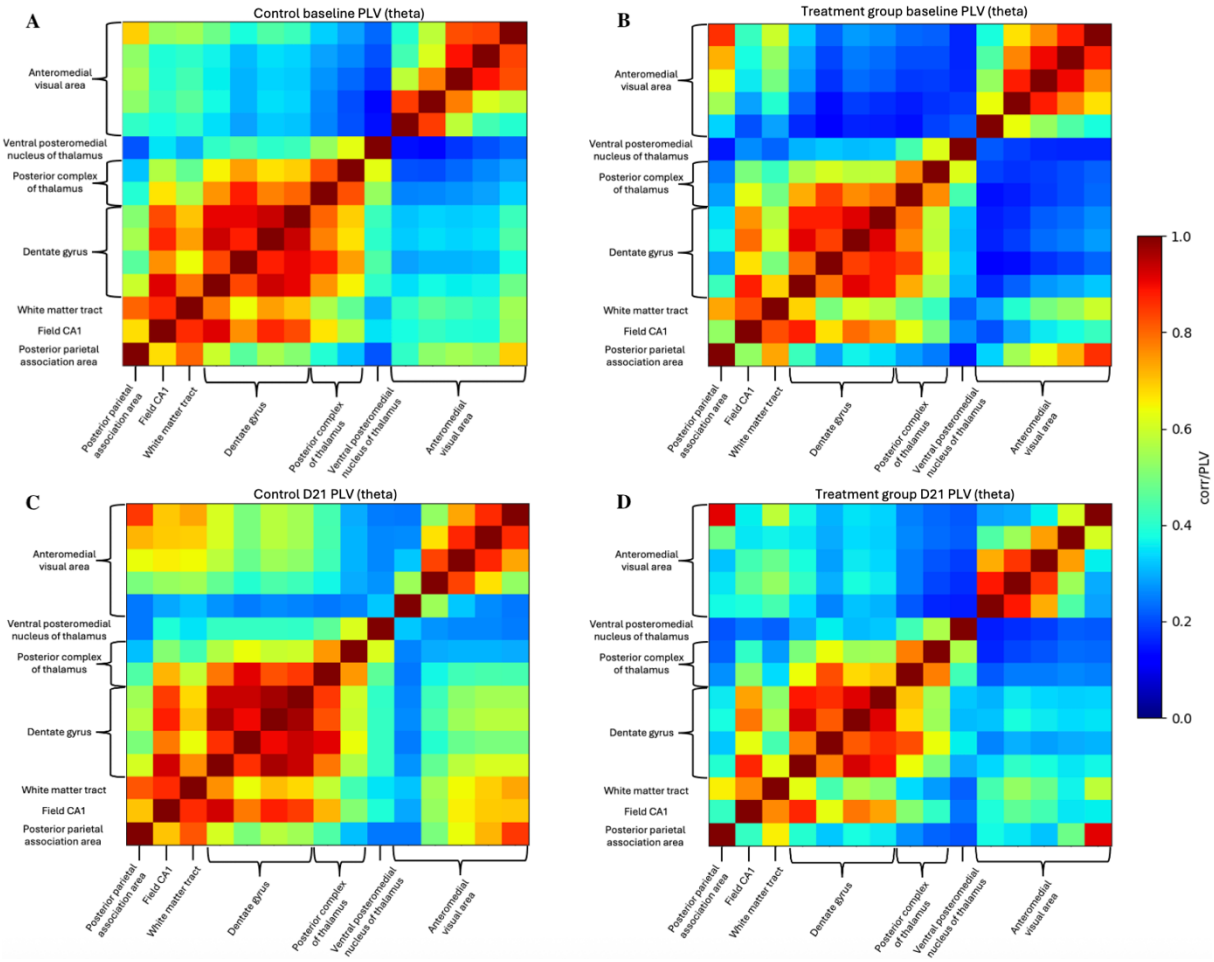

Figure 3. Phase locking values of the caudal Neuropixels electrode in theta frequency (4-8 Hz). Sections A and C include the baseline and post-21-days values of the control group (n = 3), and sections B and D include the baseline and post-treatment values of the treatment group (n = 3). In control group, the anteromedial visual area layers express a slight increase in phase synchrony from 0.5 to 0.7 whereas otherwise the values remain similar between baseline and post-21-days. In the treatment group, a similar increase can be seen in the anteromedial visual area layers but in some thalamic and hippocampal areas there is a slight decrease of approximately 0.3 units. Additionally, the synchrony within the anteromedial visual area layers decreases slightly.

In figure 4A and 4C, consisting of the recordings from the control group, a similar change in the synchrony of anteromedial visual area can be seen as in the theta band. Otherwise, the synchrony within the control group remains relatively unchanged. In 4B and 4D, showing the treatment group, the changes between the baseline and post-treatment, follow similar pattern as in the theta band. Within the anteromedial visual area, the synchrony between different layers seems to decrease and the synchrony between thalamic and hippocampal areas decrease slightly.

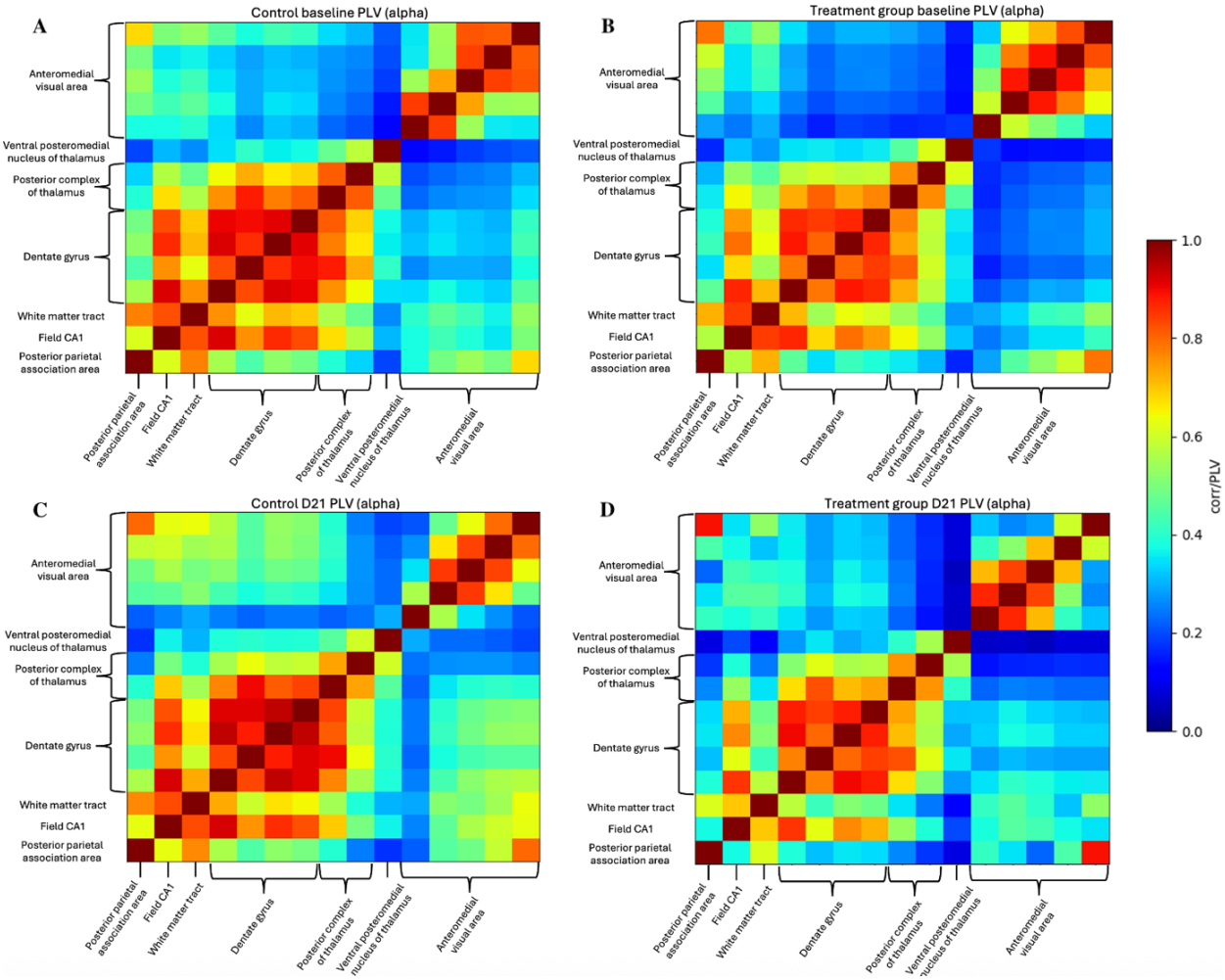

Figure 4. **Phase locking values of the caudal Neuropixels electrode in alpha frequency (8-12 Hz).** Sections A and C include the baseline and post-21-days values of the control group (n = 3), and sections B and D include the baseline and post-treatment values of the treatment group (n = 3). Similarly to theta, there is a slight increase in the control group's anteromedial visual area layers between A and C, which can also be observed in the treatment group between sections B and D. Also, between B and D there is a decrease within the anteromedial visual area layer and between certain thalamic and hippocampal areas.

Figures 5 and 6 show the phase locking value (PLV) synchronization heatmaps of the theta (Figure 5) and alpha (Figure 6) bands from the rostral Neuropixels electrode. Again, sections A and B represent the baseline values of the control group and treatment group, respectively. Similarly, sections C and D show values from the second recording after the 21-day period, with C showing the control group and D showing the treatment group.

In the rostral regions the baseline activity is much higher in both theta and alpha bands throughout the whole heatmap. In theta, the control group shows minimal changes between the baseline (5A) and post-21-days (5C), with the most noticeable changes in the olfactory areas, a region not related to the DMN. In the treatment group, the synchrony increases in the area consisting of secondary motor area layers, infralimbic area layers, and the anterior cingulate

area between the baseline (5B) and post-treatment (5D) recordings. Otherwise, the synchrony remains relatively unchanged with some individual exceptions in the prelimbic area layers.

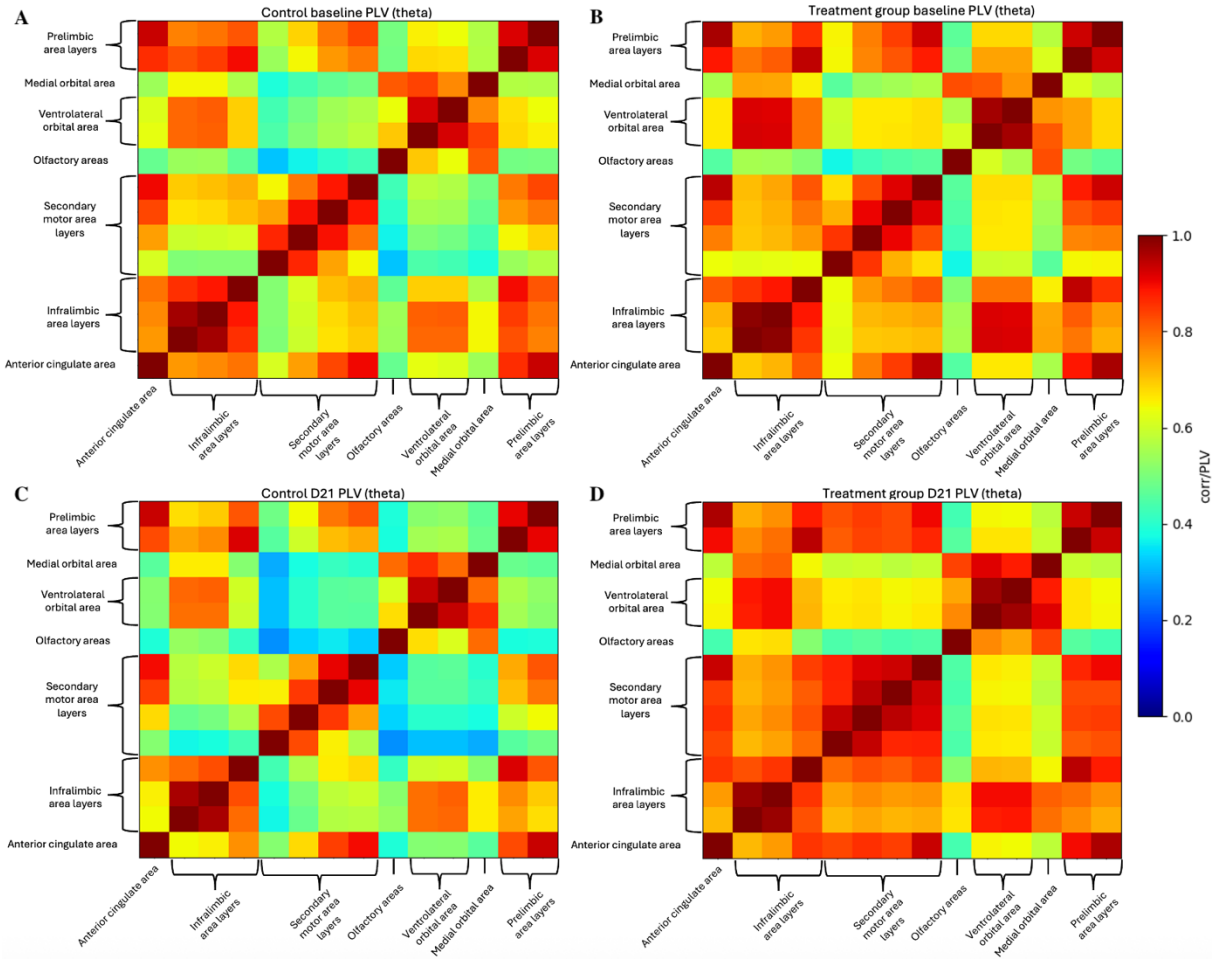

Figure 5. **Phase locking values of the rostral Neuropixels electrode in theta frequency (4-8 Hz).** Sections A and C include the baseline and post-21-days values of the control group (n = 3), and sections B and D include the baseline and post-treatment values of the treatment group (n = 3). Values in control group between A and C remain relatively unchanged. In the treatment group, between B and D, the values increase approximately by 0.25 in prelimbic area layers, secondary motor area layers, infralimbic area layers, and anterior cingulate area. Also, the synchrony within the orbital area layers increases between B and D.

The alpha band in figure 6 follows the same pattern as theta in figure 5. The control group shows again only slight differences between baseline recording (6A) and post-21-days recording (6C). In the treatment group, a slightly more intense increase in synchrony can be seen in the post-treatment group (6D) when comparing to the baseline values (6B). Especially in the area consisting of the secondary motor area layers, infralimbic area layers, and anterior cingulate area, the synchrony becomes heightened. Additionally, the increase in some of the prelimbic area layers seems more intense in alpha band, than in theta band.

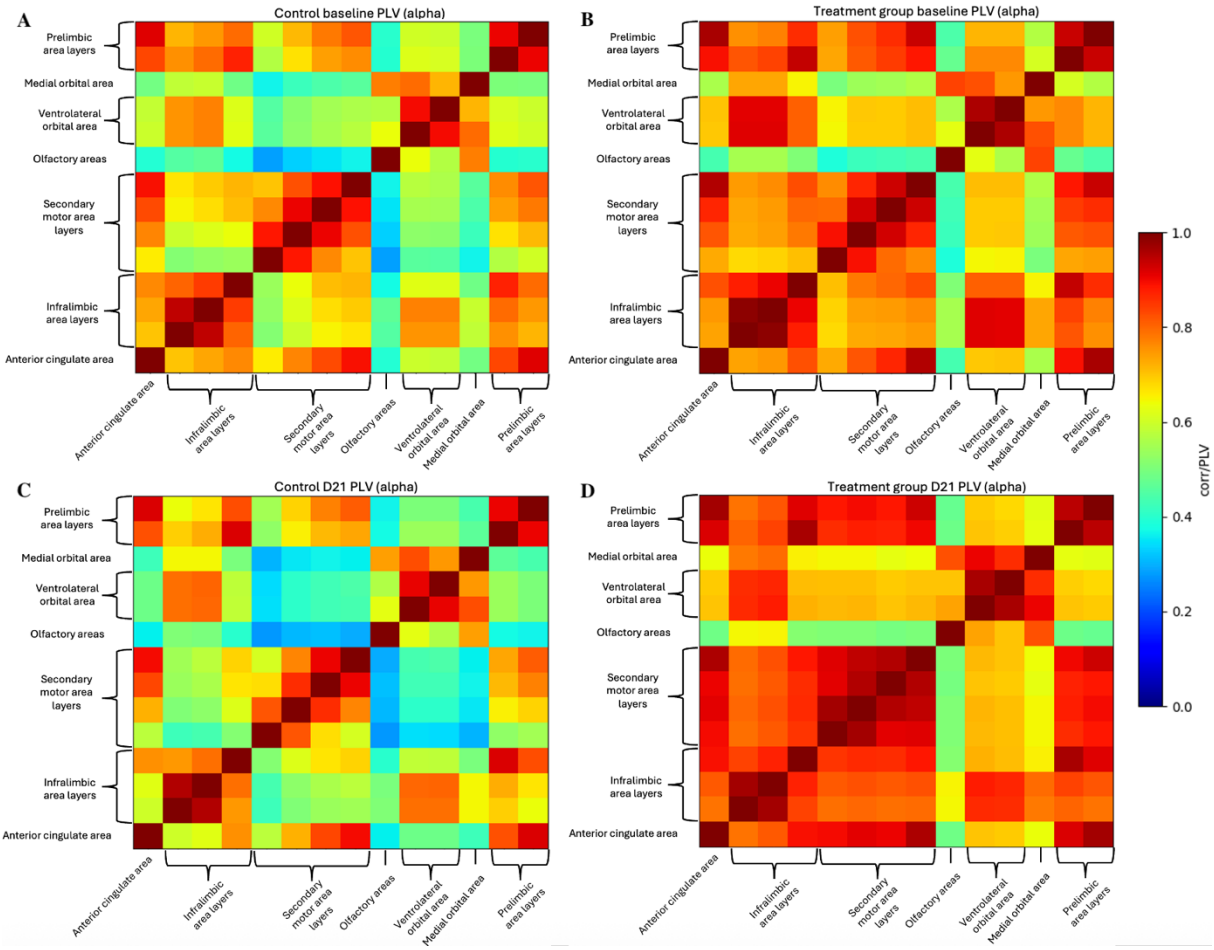

Figure 6. **Phase locking values of the rostral Neuropixels electrode in alpha frequency (8-12 Hz).** Sections A and C include the baseline and post-21-days values of the control group (n = 3), and sections B and D include the baseline and post-treatment values of the treatment group (n = 3). Values in control group between A and C remain similar. In the treatment group the values increase in similarly as in the theta frequency including the prelimbic area, orbital area layers, secondary motor area layers, infralimbic area layers, and anterior cingulate area.

2.1.2 Dynamic functional connectivity

In figure 7 and 8 are the results from the dynamic functional connectivity (DFC) analysis describing how the connectivity changes over time. Values from figure 7 are from the caudal Neuropixels electrode and values from figure 8 are from the rostral Neuropixels electrode. In both figures sections A and B describe the baseline values from control (n = 3) and treatment groups (n = 3), respectively, whereas sections C and D describe the post-21-days values from the control and treatment groups, respectively.

In figure 7 showing the DFC values of the caudal regions, a slight variability in the control group can be seen between the baseline (7A) and post-21-days (7C). Most noticeable changes can be seen in the thalamic areas, that seem to have an increase in DFC between the timepoints. Additionally, the anteromedial visual area shows decreases in DFC especially with the area

itself, but also with some other areas. However, overall connectivity patterns remain similar between baseline and post-21-days. In the treatment group, the baseline DFC values (7B) are slightly higher but looking at the post-treatment values (7D), there is a large decrease in the values throughout the whole heatmap. Only few individual areas remain at similar values between baseline and post-treatment timepoints showing a clear decrease in the caudal DFC.

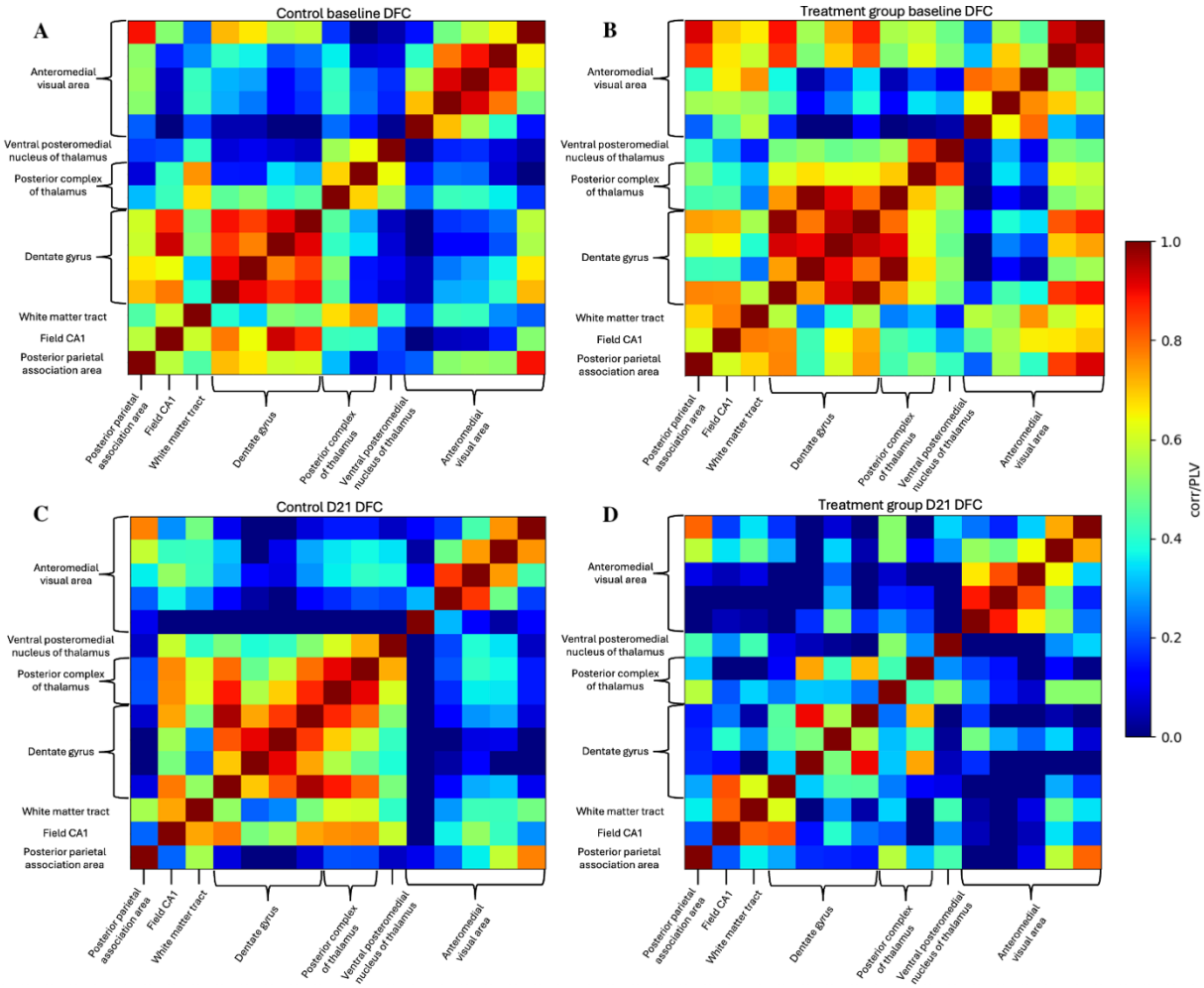

Figure 7. **Dynamic functional connectivity values of the caudal Neuropixels electrode.** Sections A and C include the baseline and post-21-days values of the control group (n = 3), and sections B and D include the baseline and post-treatment values of the treatment group (n = 3). In the control group there are small differences in the DFC between A and C, but the overall level remains at moderate. In the treatment group the difference between B and D is much more evident where the DFC decreases almost totally throughout the caudal regions. Only within the anteromedial visual area layer there remains moderate values of DFC in the post-treatment group.

Figure 8, consisting of the rostral DFC values, shows extremely heightened values already in the baseline timepoints both in control group (8A) and treatment group (8B). However, the control group has a few regions showing lower values whereas the treatment group shows lower values only in the olfactory area. After the 21-day period, the values from the control group (8C) are slightly lower and the variability looks more normal. Additionally, the patterns of the

DFC follows similar pattern as the PLV control group, shown in figure 6C. In the treatment group, the trend of excessive DFC values persists to the post-treatment period (8D) as well. Despite of this excess activity, the area consisting of secondary motor area layers, shows slightly increased values when compared to the baseline whereas the rest of the heatmap is closely similar to the baseline values.

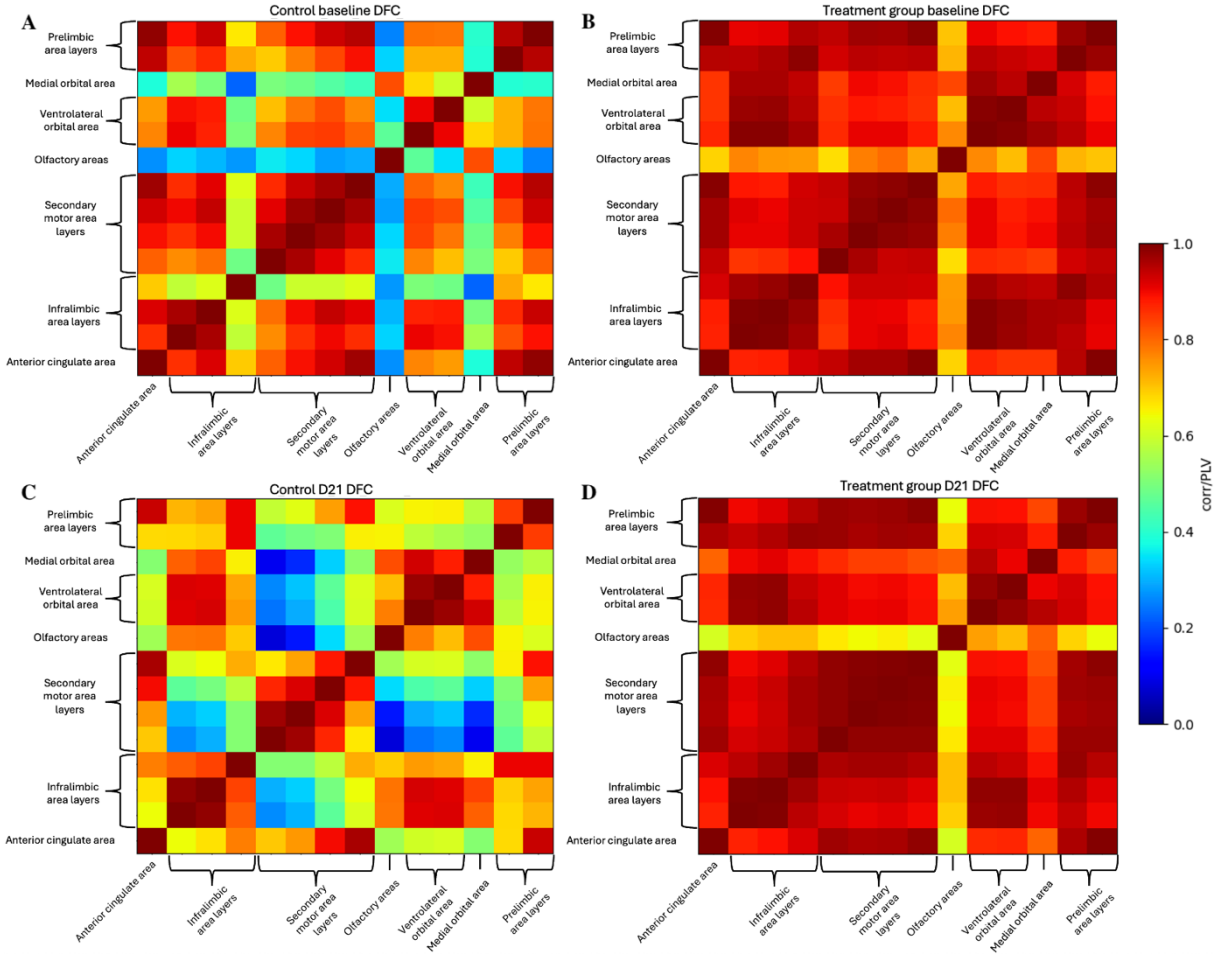

Figure 8. **Dynamic functional connectivity values of the rostral Neuropixels electrode.** Sections A and C include the baseline and post-21-days values of the control group (n = 3), and sections B and D include the baseline and post-treatment values of the treatment group (n = 3). Both baseline values in A and B show excessive DFC values, although the control group has slightly more variation to its values. Also, in the post-21-days of the control group the values are much more moderate and show more normal DFC between regions. However, in the post-treatment group (D), the values are even more excessive than in the baseline, especially in the secondary motor area layers and infralimbic area layers.

2.1.3 Amplitude correlation analysis

Figures 9 and 10 show the values from the amplitude correlation analysis (ACA) from the caudal and rostral Neuropixel electrodes, respectively. Sections A and B represent the baseline values of the control group (A) and treatment group (B). Similarly, sections C and D show values from the second recording after the 21-day period, with C showing the control group (n

= 3) and D showing the treatment group (n = 3). The scalebar on the right shows that higher values, that indicate higher correlation, are depicted in deeper purple and smaller values, indicating negative correlation between regions, are depicted in orange. The ACA values from the caudal electrode in figure 9 show higher correlation values (0.75-1.00) within the thalamic and hippocampal areas, as well as within the anteromedial visual area. Otherwise, the amplitude correlation remains around 0.25. In the treatment group there is not any evident differences between baseline and post-treatment values, and the control group and treatment group values are fairly similar to each other.

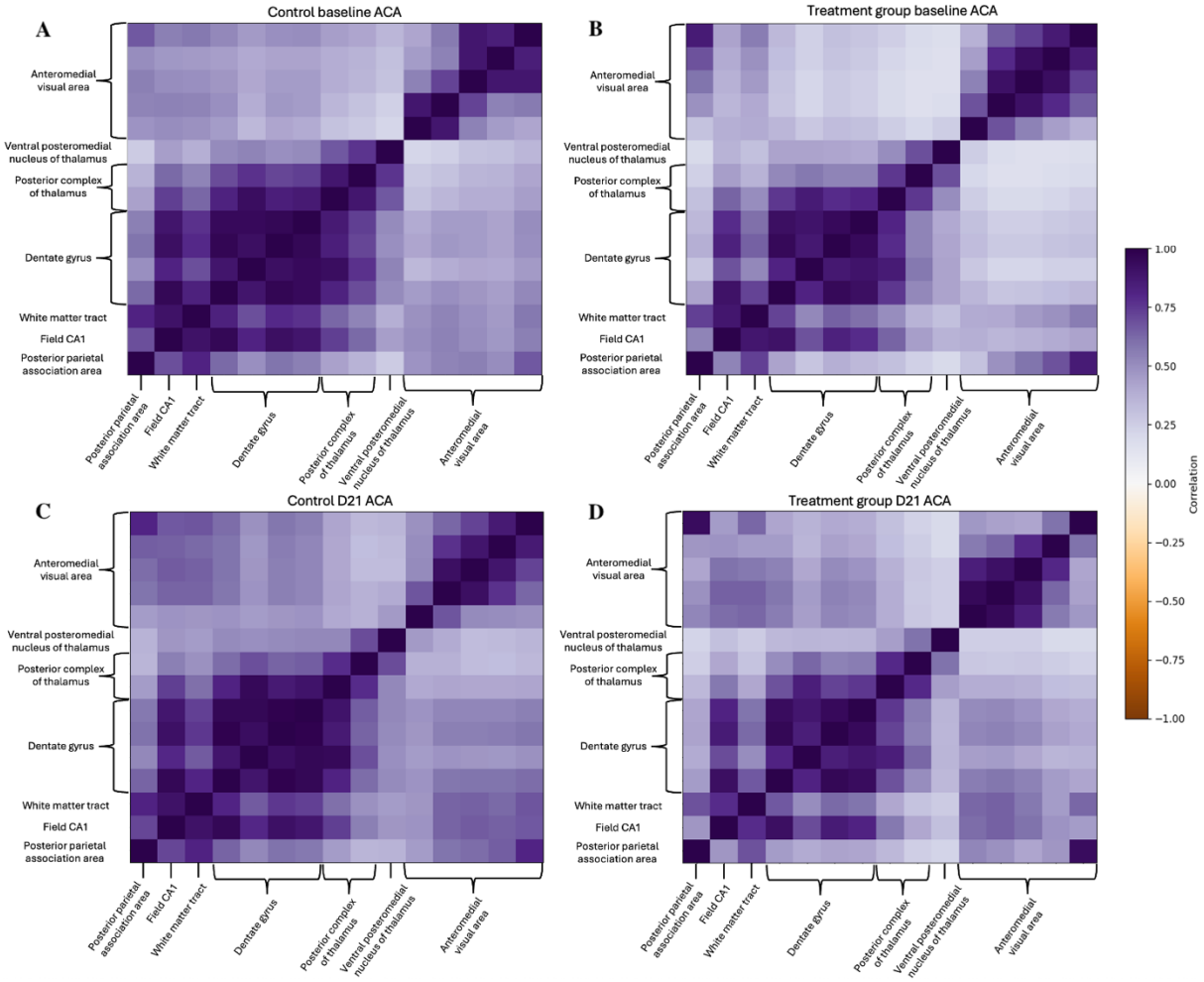

Figure 9. **Temporal amplitude correlation values of the caudal Neuropixels electrode.** Sections A and C include the baseline and post-21-days values of the control group (n = 3), and sections B and D include the baseline and post-treatment values of the treatment group (n = 3). In the control group there is not any evident differences between baseline (A) and post-21-days (C) values. Also, in the treatment group, the amplitude correlation remains at similar values at respective locations. Overall, the amplitude correlation is higher in thalamic and hippocampal areas as well as in the anteromedial visual area layers with values between 0.75-1.00. Otherwise, the correlation is slightly positive with values over 0.25.

In figure 10, consisting of ACA values from the rostral electrode, the overall amplitude correlation seems to be slightly higher throughout the regions of interest, with values ranging mostly from 0.50 to 1.00. Again, no evident differences can be seen in the amplitude correlation between baseline and post-treatment recordings, apart from small increase in the secondary motor area layers and infralimbic area layers. Also, in the control group there is a slight decrease in the overall correlation strength with values decreasing around 0.25 in most parts. However, in orbital area layers, infralimbic area layers, and secondary motor area layers the values persist similar to baseline values. No negative correlation was observed in neither, caudal nor rostral electrodes.

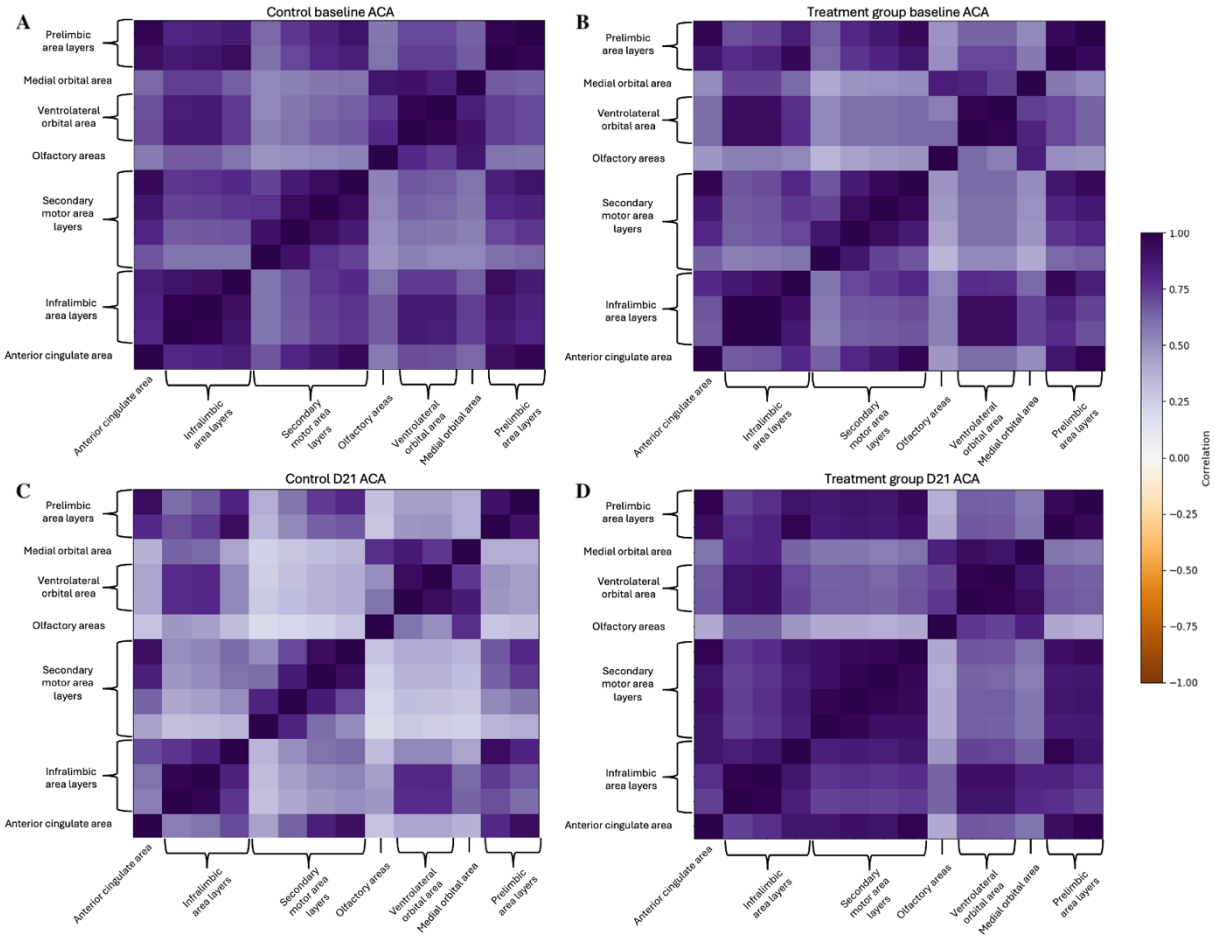

Figure 10. **Temporal amplitude correlation values of the rostral Neuropixels electrode.** Sections A and C include the baseline and post-21-days values of the control group (n = 3), and sections B and D include the baseline and post-treatment values of the treatment group (n = 3). The overall baseline correlation is higher than in the caudal regions with values mostly over 0.50. In the control group the correlation decreases between baseline (A) and post-21-day (C) values overall around 0.25 units although the correlation persists more notably within the secondary motor area layers, infralimbic area layers, and orbital area layers. In the treatment group the amplitude correlation remains quite similar between baseline (B) and post-treatment (D) values, although there is a slight increase in the secondary motor area layers and infralimbic area layers.

2.2 µECoG-grids

2.2.1 Phase locking value

Figures 11 and 12 show the phase locking value (PLV) synchrony heatmaps of the theta (4-8 Hz) (Figure 11) and alpha (8-12 Hz) (Figure 12) bands from the cortical µECoG-grids. In both figures, sections A and B represent the baseline values of the control group (n = 3) (A) and treatment group (n = 3) (B). Similarly, sections C and D show values from the second recording after the 21-day period, with C showing the control group and D showing the treatment group. The scalebar on the right shows that higher values, which indicate more synchronous connections, are depicted in warmer colours (red) and smaller values, indicating less synchrony between regions, are depicted in colder colours (blue). In figure 11, depicting the theta phase locking values of the control group, the PLV remains low with the baseline values being mostly around 0.0-0.3 and the values from post-21-days recording being between 0.0-0.4. Only exception is the synchrony between right and left retrosplenial cortices (Rsp) which remain at high synchrony (0.8-0.9) in each time point and study group. Additionally, the synchrony of the left anterior cingulate cortex (ACC) with other regions of interest increases slightly to 0.4. In the treatment group, the baseline values are increased clearly up to 0.7 when comparing to the control group, but in the post-treatment recording the values decrease visibly back to similar values as in the control group.

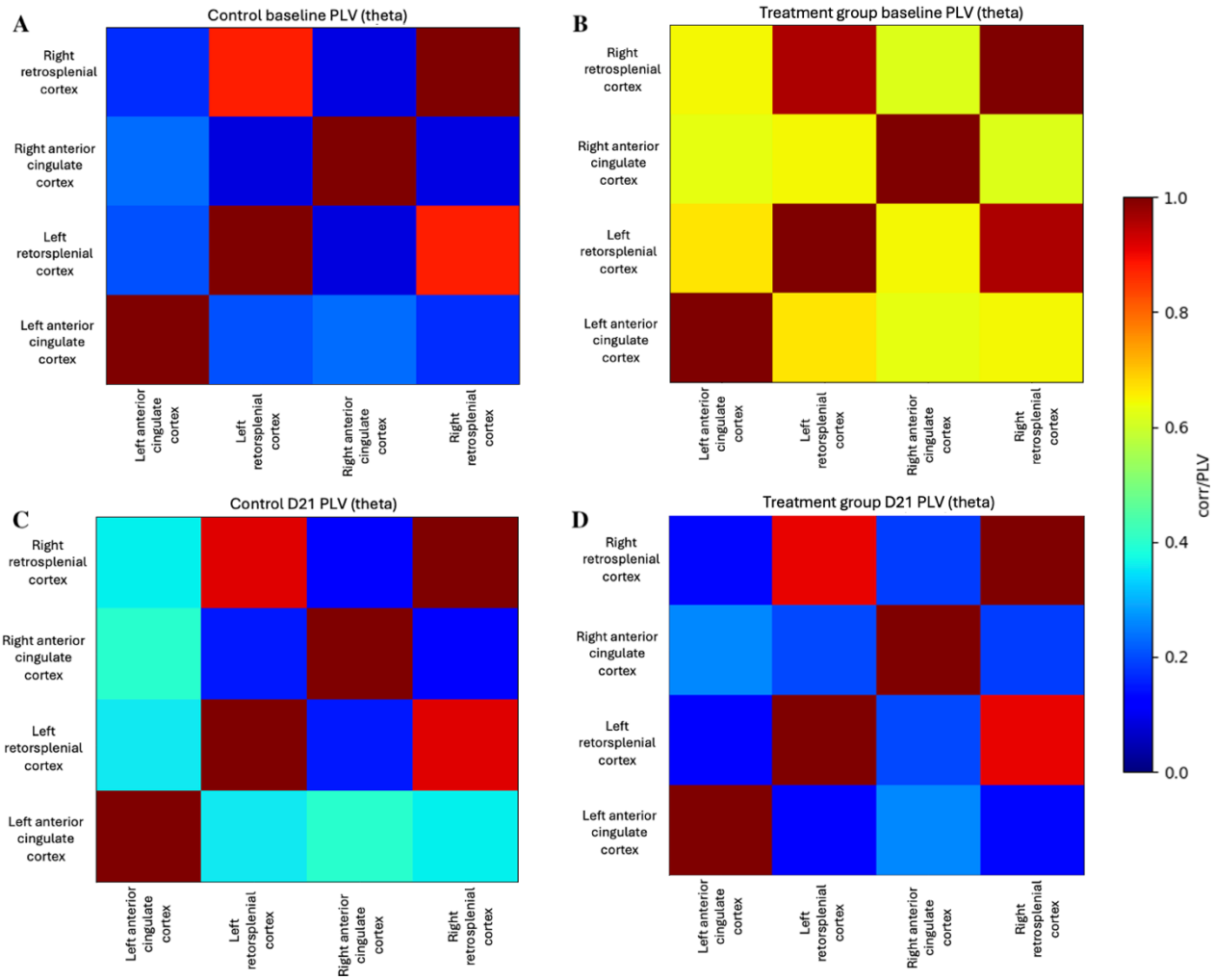

Figure 11. Phase locking values of the µECoG-grids in theta frequency (4-8 Hz). Sections A and C include the baseline and post-21-days values of the control group (n = 3), and sections B and D include the baseline and post-treatment values of the treatment group (n = 3). Between the timepoints of control group (A, C), the only difference is the slight increase of synchrony between the left anterior cingulate cortex and other regions of interest in the post-21-days values (C). Otherwise, the synchrony is overall low apart from the synchrony between left and right retrosplenial cortices. In the treatment group, the baseline synchrony (B) is clearly higher with values around 0.7 but this synchrony decreases in the post-treatment group (D) back to similar values as in the control group around 0.2.

Similarly to figure 11, figure 12 shows only a little change between the different timepoints of the control group whereas the baseline values of the treatment group are visibly higher (0.5-0.7) and decrease clearly in the post-treatment values back to similar values as in the control group (0.0-0.2). In the control group left ACC shows again increased synchrony with other regions of interest, although less prominent.

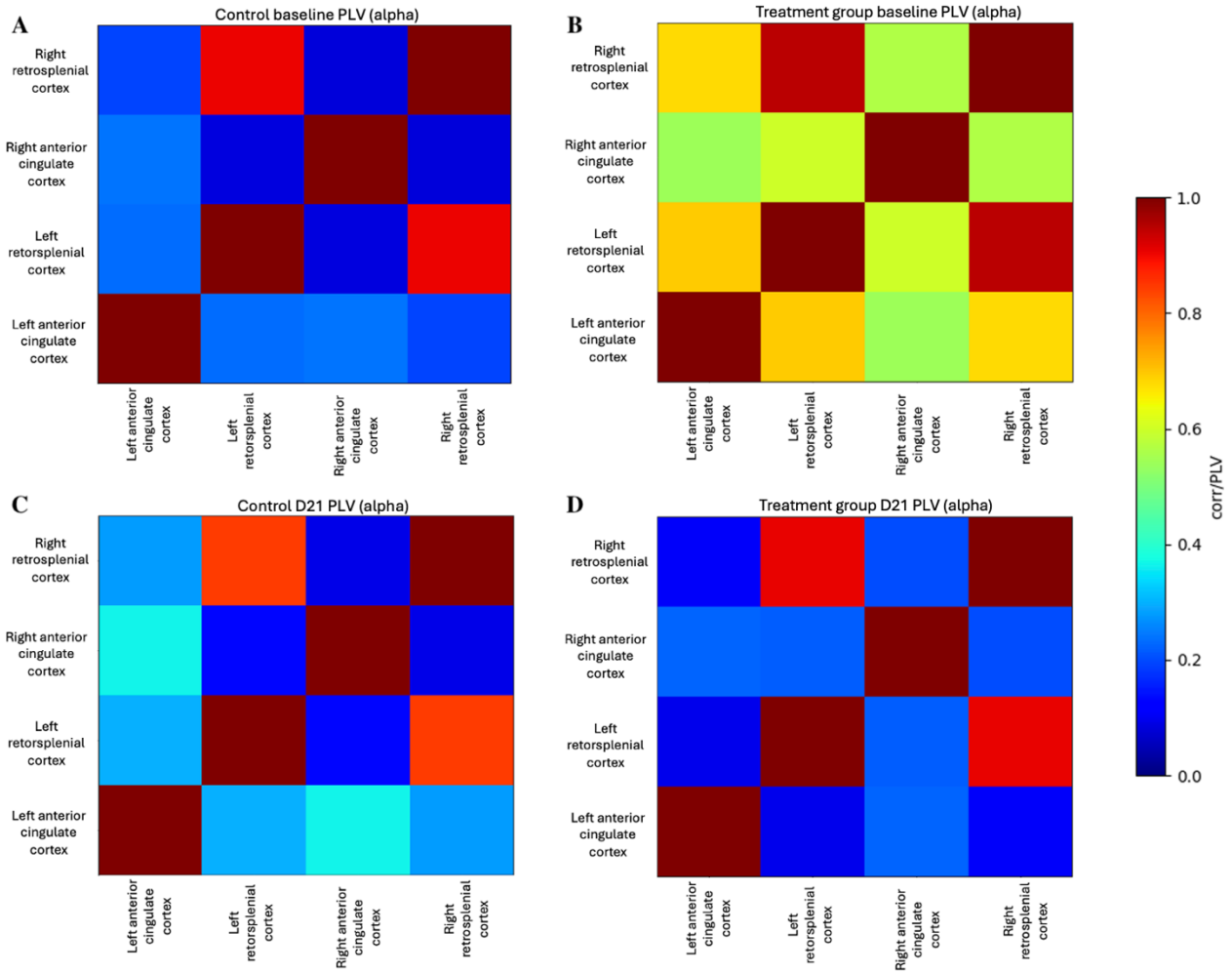

Figure 12. **Phase locking values of the µECoG-grids in alpha frequency (8-12 Hz).** Sections A and C include the baseline and post-21-days values of the control group (n = 3), and sections B and D include the baseline and post-treatment values of the treatment group (n = 3). As in the theta frequency, the synchrony of the control group remains low in alpha frequency as well between the baseline (A) and post-21-days (C). Also, in the treatment group similar trend can be seen where the baseline (B) is evidently higher with values around 0.7 that decrease in the post-treatment (D) values into similar values as in the control group around 0.2. In each group, the synchrony between left and right retrosplenial cortex remains high.

2.2.2 Dynamic functional connectivity

Figure 13 shows the DFC values from the cortical µECoG-grids. Sections A and B show the baseline values of the control group (A) and treatment group (B), and sections C and D show the post-21-days values of the control group (n = 3) (C) and treatment group (n = 3) (D). In the control group the DFC stays low (0.2-0.4) within the left anterior cingulate cortex in both timepoints but the DFC in other areas is relatively high (0.6-0.8). In the treatment group the baseline values are slightly higher within the left anterior cingulate cortex (0.4-0.5) than in the control group, and other regions show similar values as control group's baseline although slightly lower (0.45-0.75). In section D the overall values are, however, much lower (0.1-0.3)

apart from the DFC between the different hemispheres of Rsp and ACC, which still express high values (0.75-0.9).

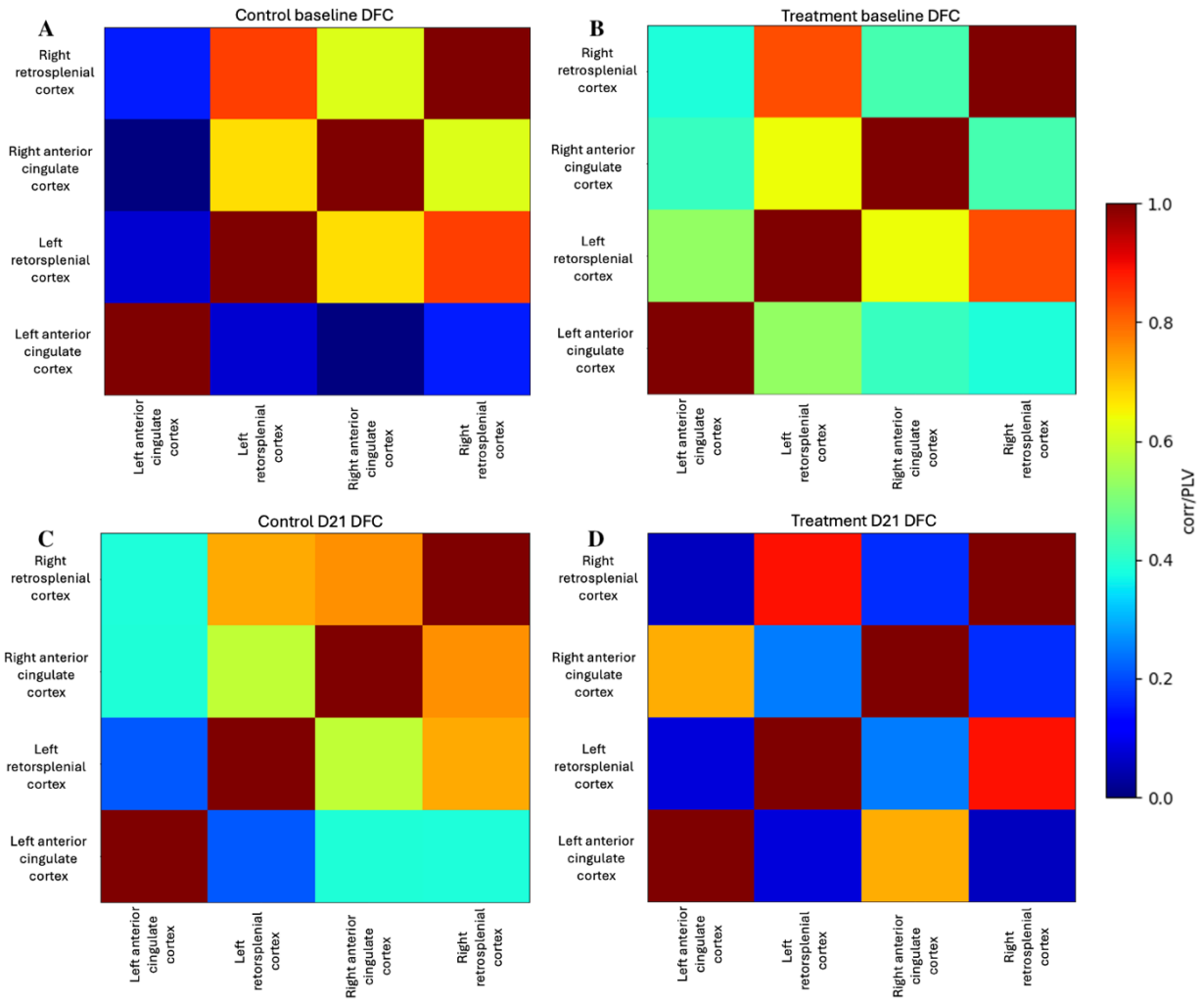

Figure 13. **Dynamic functional connectivity values of the µECoG-grids.** Sections A and C include the baseline and post-21-days values of the control group (n = 3), and sections B and D include the baseline and post-treatment values of the treatment group (n = 3). In the control group, the baseline (A) and post-21-days (C), show similar values, where left anterior cingulate cortex shows little DFC, although it increases in the section C, and other regions show higher values. The treatment group's baseline (B) values are slightly higher but similar to control group's post-21-days values, but in the post-treatment (D) values the DFC is overall low with exceptions in the DFC of right anterior cingulate cortex and left anterior cingulate cortex and between right and left retrosplenial cortices.

2.2.3 Amplitude correlation analysis

In figure 14 are the values from the amplitude correlation analysis (ACA) from the cortical µECoG-grid. In sections A and B are the baseline values of the control group (n = 3) (A) and treatment group (n = 3) (B), and sections C and D show values from the second recording after the 21-day period, with C showing the control group and D showing the treatment group. The scalebar on the right shows that higher values, that indicate higher correlation, are depicted in deeper purple and smaller values, indicating negative correlation between regions, are depicted

in orange. Overall, the amplitude correlation remains extremely high throughout all the different sections (A-D) with correlation values ranging from 0.75 to 1.0. In the treatment group there is a slight decrease in ACA values between the Rsp (caudal) and ACC (rostral) from 0.9 to 0.75.

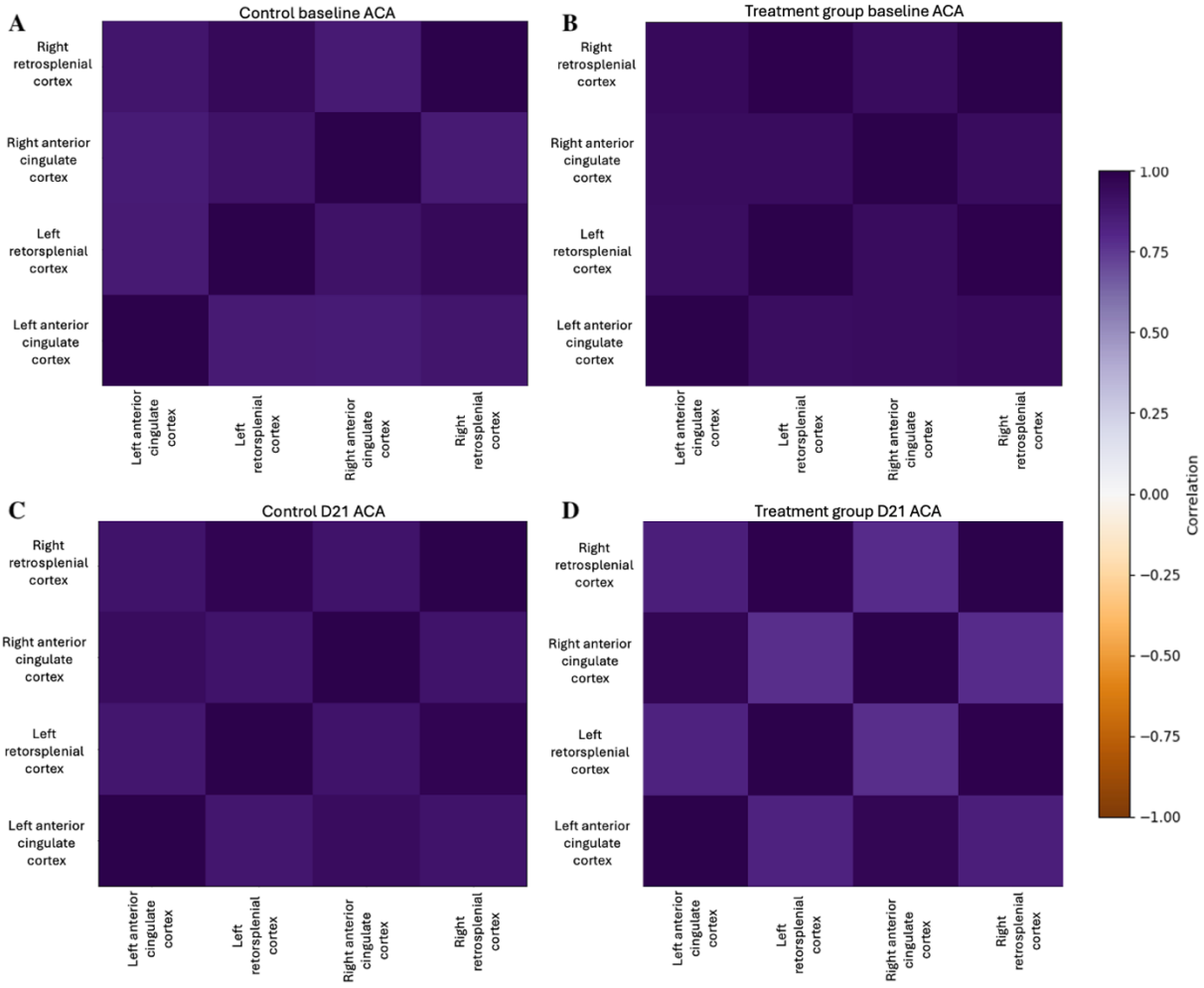

Figure 14. **Temporal amplitude correlation values of the µECoG-grids.** Sections A and C include the baseline and post-21-days values of the control group (n = 3), and sections B and D include the baseline and post-treatment values of the treatment group (n = 3). The ACA values are extremely high in both, control group and treatment group, and in both, baseline and post-21-days values. All the values are around 0.75-1.00 and no clear changes can be seen between the timepoints apart from the slight decrease in the treatment group between the retrosplenial cortices and anterior cingulate cortices.

3 Discussion

The default mode network has been characterised to be a central network in the pathophysiology of depression, but previous studies have mostly focused on the human DMN (Kaiser et al., 2015). However, regarding the development of novel drugs, animal models remain irreplaceable. Therefore, the understanding of neural functionality in animals and translational possibilities to humans needs to be expanded. The aims of this thesis were to study the default mode network in a mice depression animal model to gain more knowledge of the DMN's activity and functional connectivity in both healthy control mice and mice with depression-like characteristics. Additionally, the aim was to study the oscillatory synchrony dynamics within the DMN to understand their role in depression pathology better.

By performing a large craniotomy surgery and by utilizing a novel electrophysiological setup consisting of two intracranial Neuropixels electrode probes and two cortically placed micro-electrocorticography grids targeting the DMN, the neural activity of this resting-state network was captured successfully. However, due to the restricted timeframe of this thesis, we managed to produce a total sample size of only 6 mice. Therefore, the results of this thesis need to be interpreted carefully, and no definitive conclusions can be made. By inducing depression-like characteristics with chronic corticosterone administration via drinking water, the possible pathological changes of depression were also studied to some extent. Although this pharmacologically induced depression model is previously validated, it is not the most used in depression research and holds some flaws (Planchez et al., 2019). However, due to the intensity of the surgeries, other, more common depression animal models, were ruled out in order not to harm the animals. Despite of this, no behavioural testing was done in this thesis to further validate the used model. What adds weight to the lack of behavioural testing is that the mice were all females, and housed individually after the surgeries, possibly affecting the control group's phenotype as well, due to females being more susceptible to social stress (Takahashi et al., 2017). Therefore, it would be important to implement behavioural testing to the study protocol to confirm the depressive phenotype in the treatment group. Nevertheless, these issues were addressed to some extent by using each mouse as their own control by performing a baseline recording before the treatment period.

Regarding the phase locking value, this thesis shows that in the caudal intracranial areas (figures 3 and 4), the synchrony is highest between the thalamic and hippocampal regions as well as within the anteromedial visual area, all of which are regions related to the DMN. In the

treatment group the connections between these regions seem to however decline slightly suggesting a possible decrease in the communication of these areas in the state of induced depression. In human studies alterations in functional connectivity of the thalamus and hippocampus have been constant in MDD patients although the results have been variable, showing both, increases and decreases in the connectivity (Kaiser et al., 2015; Mulders et al., 2015). The variation in the previously observed changes of functional connectivity could be due to individual variability or dependent on the depression subtype. Therefore, alterations in the synchrony would be expected as was shown is this thesis, but the direction of the change would depend on the study type and population, meaning that comparison to other studies would not be straightforward. As the theta and alpha frequencies are most reported to be altered in depression, only their results were implemented in this thesis (Fernández-Palleiro et al., 2020). However, delta (0.5-4 Hz), beta (12-35 Hz), and gamma (35-90 Hz) frequencies followed similar patterns as alpha and theta in the phase locking value which can be seen in appendices 1, 2, and 3.

In the rostral areas (figures 5 and 6), the synchrony was reported as the highest in the secondary motor area layers and infralimbic area layers. Also, the overall synchrony was higher in these rostral areas. Contrary to the caudal areas, there was an increase in the PLV in the treatment group, especially in the areas consisting of secondary motor area layer and infralimbic layer, but also in the prelimbic layers. These regions are all associated closely with the DMN, so the synchrony within the frontal DMN seemed to increase slightly. As mentioned before, many previous studies have reported alterations in the DMN functionality with variable results. Furthermore, a common finding is a possible dissociation between the frontal and posterior regions of the DMN, which could explain the different alterations in the caudal and rostral sections (Mulders et al., 2015). The connectivity between these regions were not however directly measured from the intracranial electrodes, so no conclusions can be made from this result regarding the front-back connectivity. Nevertheless, the PLV from the cortical µECoG-grids show a clear decrease in synchrony between rostral ACC and caudal Rsp areas in the treatment group (figures 11 and 12), also suggesting a dissociation between frontal and posterior DMN regions. However, the results from the µECoG-grids have a lot of variation, and the baseline values of the treatment group, are the only values showing higher synchrony whereas, all other µECoG PLVs, including the control group and the post-treatment values, are low. Therefore, although dissociation is commonly reported between front and back DMN regions, no definitive conclusions can be made from these results. Additionally, the anterior and

posterior regions differ in their specific tasks with the anterior regions being more related to regulation of emotions and self-referential thinking, and the posterior regions being more related to memory processing and consciousness (Mulders et al., 2015). Therefore, these regional differences in tasks could also explain the different responses to induced depression-like characteristics between frontal and posterior areas.

So, although recordings were performed in mice, the results from the PLV in this thesis suggest an increase in the frontal synchrony possibly leading to more self-referential ruminative thinking patterns. Also, the decrease in the synchrony of the posterior areas could possibly be related to impaired memory processing and attention control. However, due to the small sample size, no final conclusions can be drawn, and the results need to be confirmed with a larger sample size. Also, as the DMN regions between humans and mice are not equal, it would be beneficial to compare these results with equal human EEG/MEG recordings from MDD patients to further validate the structure of mouse DMN. Ultimately, understanding the functionality and the translational value of the mouse DMN in depression would be important when developing novel antidepressants.

This thesis also investigated how the functional connectivity changes over time with the dynamic functional connectivity (DFC) analysis. The DFC shows how much the connectivity varies during a certain timeframe suggesting how flexible or rigid the network is. Commonly MDD is associated with more rigid network dynamics which would be seen as lower DFC values but again, results regarding the functional connectivity have been contradicting (Hamilton et al., 2011; Wise et al., 2017). Here the data from the treatment group shows, that in the caudal intracranial regions, the DFC decreases drastically throughout all the targeted brain areas suggesting a more rigid dynamic functional connectivity in depressed individuals (figure 7). This aligns with previous studies regarding the DMN's functional connectivity possibly relating to common symptoms observed in depression such as impaired memory and decreased information processing of past and future events, as the dynamic properties of the DMN are reduced (Gozzi & Zerbi, 2023; Grandjean et al., 2016; Yan et al., 2019). In the rostral areas, the values of the treatment group are extremely high in both baseline and post-treatment figures (figure 8). Despite of the post-treatment values being slightly higher than the baseline, suggesting an increase in DFC, it is likely that the signal has been disrupted or that there has been an error in the data analysis resulting in these excessive values in the rostral DFC. However, if the increase is true in the post-treatment values, it would suggest that the rostral areas, responsible for higher order cognitive functions in humans, become hyperflexible in

depression possibly accounting for excessive ruminative thinking patterns and maladaptive self-focus, which has been hypothesised previously as well in depression (Hamilton et al., 2015). Additionally, in the cortical data (figure 13), a decrease in the DFC can be seen between the front and back regions, suggesting a more rigid functional connectivity between the anterior and posterior areas of the DMN. This adds further validity to the hypothesis of front-back dissociation of the DMN in depression. However, in future studies, additional care needs to be taken when analysing the data to identify possible flawed data and the results need to be confirmed with a larger sample size to provide some statistical power to the results.

Lastly, to see how the amplitude correlates between brain regions, and whether it expresses any changes after the treatment, the amplitude correlation analysis (ACA) was performed. Stronger amplitude correlation suggests more synchronized neural activity between different brain regions in terms of amplitude. In depression, within the DMN, as the overall activity is thought to increase in the frontal areas, possibly leading to rumination, and to decrease in the posterior areas, possibly leading to impaired memory and attention control, it would be expected that the amplitude correlation would react in these areas in a similar trend (Kaiser et al., 2015). However, there was not any noticeable changes observed in the ACA. In the caudal regions (figure 9), the ACA values remain unchanged between the baseline and post-21-days. On the other hand, in the rostral regions (figure 10), although there is a slight increase especially in the secondary motor area layers and the infralimbic area layers, it is approximately of the same magnitude as the decrease between the timepoints in the control group. In the cortical areas (figure 14), there is a slight decrease in the treatment group between the rostral and caudal areas, and the correlation between left and right hemispheres remains at high values. This slight cortical front-back decrease could support the hypothesis of disconnection between anterior and posterior DMN regions, but again, due to small sample size, no definitive conclusions can be made. Overall, these results showed that ACA does not seem to be affected noticeably in the intracranial areas, although changes in amplitude correlation are a relatively common finding in MDD patients (Sihn et al., 2023).

In addition to the previously mentioned limitations of small sample size, lack of behavioural testing, and all mice being female, this thesis had certain limitations. One major issue was that the trajectories of the intracranial Neuropixels probes were not confirmed during this study. Although the probes were placed with a stereotactic frame with definitive markings where to enter the brain, it is possible that the probes were not in the desired regions targeting the DMN. Therefore, the results could depict the values of other brain regions. However, as the

Neuropixels probe size is extremely small, it creates a lot of room for error in targeting the main regions of interest. Nevertheless, the trajectories need to be confirmed in future studies. Additionally, the placement of the grids was done without any definitive markings, possibly resulting into variable positioning of the grids between recordings. The placement of the grids could also be the reason for the variable results in the PLV of the μECoG (figures 11 and 12). Lastly, as the craniotomy surgery is performed around 7 days prior to the first recording, there is possibly still inflammation in the brain during the first recording which could affect the electrophysiological signal and alter the baseline values.

To conclude, by using a novel electrophysiology setup utilizing both, cortical and intracranial recording electrodes, we were able to gain more knowledge of the DMN's functionality and connectivity in both, healthy mice, and mice with depression-like characteristics. We observed a decrease of the phase synchrony within the caudal areas of the DMN whereas an increase was observed in the rostral areas. Additionally, all the results in PLV, DFC, and ACA were suggestive of a dissociation between the front and back regions of the DMN, which has commonly been hypothesised previously. Adding validity to the PLV results, the DFC showed also decreased network flexibility in the posterior regions and increased network flexibility in the anterior regions of the treatment group, suggesting a dysfunctional DMN organization. When translating results to human cognitive symptoms of MDD, these results align with commonly observed symptoms of increased ruminative thinking patterns, and decreased functionality in the memory and attention processing. However, this was a piloting study with an extremely small number of animals investigating this network at such a profound level in mice, and more research needs to be done to confirm the results. Additionally, after acquiring a larger sample size, comparing the results with equivalent human studies would provide more insights on the translational value of this study and on the organization of the mouse DMN. With further research this could provide a platform to test novel pharmacological interventions, such as derivatives of psychedelics, to see whether they could restore normal DMN functionality and flexibility in depression, in addition to their already proven plasticity inducing effects.

4 Materials and methods

4.1 Animals

In this study, we used six female wild type C57BL/6JRj mice (Janvier Labs) that were at least 13 weeks old and weighed over 20 grams. Mice were housed in individually ventilated cages in groups of 3-4 mice/cage in the laboratory animal center of university of Helsinki where they were maintained on a 12 h light/dark cycle. During housing the mice had free access to food and water *ad libitum*. Following the craniotomy surgery, the mice were moved to individual housing to avoid mice harming each other. All animal experiments were approved by the national Animal Experiment Board in Finland (license number: ESAVI/40845/2022). Experiments were conducted in compliance with the Directive 2010/63/EU of the European Parliament regarding the protection of animal use for scientific purposes, and with the institutional and national guidelines for the care and use of laboratory animals.

4.2 Craniotomy surgery

A craniotomy surgery was performed to the mice in two phases (phase A and phase B) that were 48 h apart. Both surgeries were done under isoflurane anaesthesia (Piramal Healthcare, United Kingdom), with induction in 4 % and maintenance in 1.5-2.5 %. For analgesia the mice received subcutaneous (s.c.) injections of carprofen (5 mg/kg) (Zoetis Animal Health, Belgium) and buprenorphine (0.05 mg/kg) (Indivior, USA). Additionally, 2 mg/kg of dexamethasone (Dopharma, Netherlands) was injected s.c. for anti-inflammatory purposes. The surgeries were performed on a heating pad set to 37°C and the eyes were covered with carbomer eye ointment (Viscotears, USA) and black tape for protection.

4.2.1 Phase A

Before surgery the mice were barbered from the head area and antiseptic povidone-iodine was applied to the cut area. Lidocaine-adrenaline (Lidocaine 10 mg/ml, adrenaline 10 µg/ml) (Orion Pharma, Finland) solution was injected s.c. in the head area as a local anaesthetic. The skin on top of the skull was cut with surgical scissors and the skull was exposed in an area large enough to fit a Neurotar model 13 metal headplate (Neurotar, Finland). This skull area was cleaned of excess tissue with acetone and a rectangular area in the size of 4 mm x 7.6 mm was marked on the skull with a stereotactic device. The marked area was in relation to each mouse's bregma so that the lateral sides were 2 mm from bregma on both sides, 3 mm on the rostral side, and

4.6 mm on the caudal side. Additionally, two insertion sites for Neuropixels probes were marked on the right side of the skull at 1.66 mm rostrally and 1.95 mm laterally from bregma as well as 2.2 mm caudally and 1.9 mm laterally from bregma. For recording reference signal, a hole was drilled in the skull on the left side of cerebellum area with a dental drill and a reference socket was inserted and glued in place with Loctite 401 instant adhesive glue (Henkel Adhesives, Germany). The Neurotar model 13 metal headplate was glued on top of the skull with Loctite 401 and the adhesion was strengthened with dental cement. Lastly, the mice were let to wake up from the anaesthesia and returned to their cage.

4.2.2 Phase B

In phase B, the mice received the same medications as in phase A apart from the lidocaine, and they were anesthetized with the same protocol. To create a cranial window the bone was drilled with a dental drill along the marked line on the skull that was made in phase A. Artificial cerebrospinal fluid (aCSF) was kept on ice during the surgery and applied on the surgery area regularly to keep the tissue from overheating and to restrain possible bleeding. After drilling approximately 90 % of the bone thickness the almost detached bone plate was circulated with a hook to delicately detach the bone plate from surrounding bone tissue and dura mater from beneath. Lastly, the bone plate was lifted, and the brain area was cleaned of coagulated blood with aCSF before inserting a PDMS membrane the size of the cranial window on top of the brain and sealing the opening with a silicone sealant (Kwik-Cast, World Precision Instruments, USA). To protect the cranial window during housing a 3D-printed plastic cap was glued on top of the metal headplate. Lastly, the mice were let to wake up from the anesthesia on their own on the heating pad at 37°C after which they were transferred to individual housing. Post-surgery, the health of mice was followed and when necessary carprofen was administered s.c. for analgesia for two following days.

4.3 Habituation

Before the electrophysiology recordings the mice were habituated to handling and the EEG recording platform on five separate days in increasing time lengths. For the first day they were habituated for 10 minutes followed by 20 minutes, 40 minutes, 60 minutes, and lastly 90 minutes on the fifth day.

4.4 Treatment groups

The mice were divided into two treatment groups. The first group were given 35 mg/L of corticosterone (Sigma-Aldrich, Germany) dissolved in DMSO (1 %) (Sigma-Aldrich, Germany) and water via drinking water for 21 days which they had free access to during the treatment period. The second group which was the control group were housed in regular conditions for 21 days. Both groups were housed individually after phase B surgery to avoid mice damaging each other.

4.5 Electrophysiology recordings

Following the surgery and habituation, the animals were recorded for baseline activity prior to any treatments. The recordings were performed without anesthesia on awake animals and electrophysiological data was captured at 500 Hz. During the baseline recording the mice were recorded for 30 minutes. After 21 days of corticosterone administration for the treatment group or 21 days of normal housing for the control group another EEG recording was conducted. In the recordings the mice were placed individually on the recording platform and the plastic cap, silicone sealant, and PDMS membrane were removed to expose the brain. Two µEcoG grids (NeuroNexus Technologies, USA) were placed on the cortex so that one grid was in the front and one in the backside as shown in figure 15. The areas of interest for µEcoG were the anterior cingulate cortex (ACC), secondary motor cortex, retrosplenial cortex, and the visual cortex. Additionally, two Neuropixels probes (Interuniversity Microelectronics Centre, Belgium) were placed internally in areas relevant to the DMN along trajectories that were determined in the Allen Mouse Brain Atlas with Neuropixels trajectory GUI tool. The front probe was placed 1.66 mm A/P, 1.95 mm M/L, and -50° in relevance to bregma and the back probe was placed -2.2 mm A/P, 1.9 mm M/L, and 0.90° in relevance to bregma. Neuropixels trajectories and regions of interest are provided in figure 16. The data collection from the EcoG grids and Neuropixels probes was done through the OpenEphys system using the rhythm FPGA plugin, the Neuropix-PIX plugin, and the NI-DAQMX plugin. The ages of the mice during the recordings are presented in table 2.

Table 2. Mice ages during electrophysiological recordings.

Control group			
Mouse ID	BR10	BR11	BR12
Age in 1. recording	20 weeks	20 weeks	20 weeks
Age in 2. recording	23 weeks	23 weeks	23 weeks
Treatment group			
Mouse ID	BR18	BR19	BR20
Age in 1. recording	22 weeks	26 weeks	26 weeks
Age in 2. recording	25 weeks	29 weeks	29 weeks

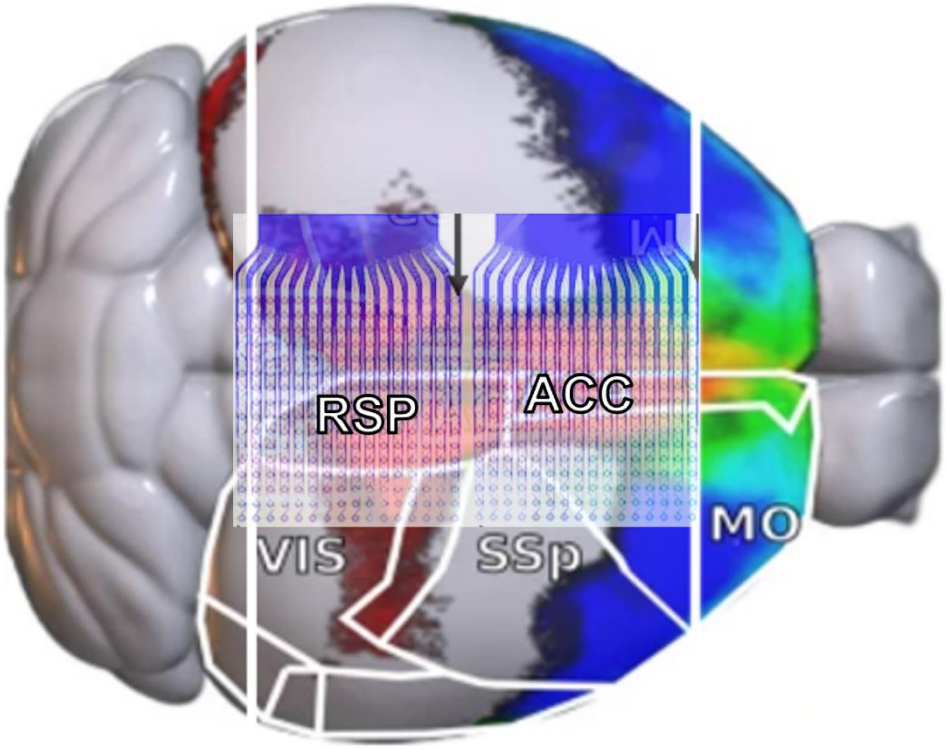

Figure 15. Placement of the electrocorticography-grids. The frontal grid was targeting the anterior cingulate cortex (ACC) and the back grid was targeting the retrosplenial cortex (RSP). Visual cortex (VIS), primary somatosensory cortex (SSp), motor cortex (MO).

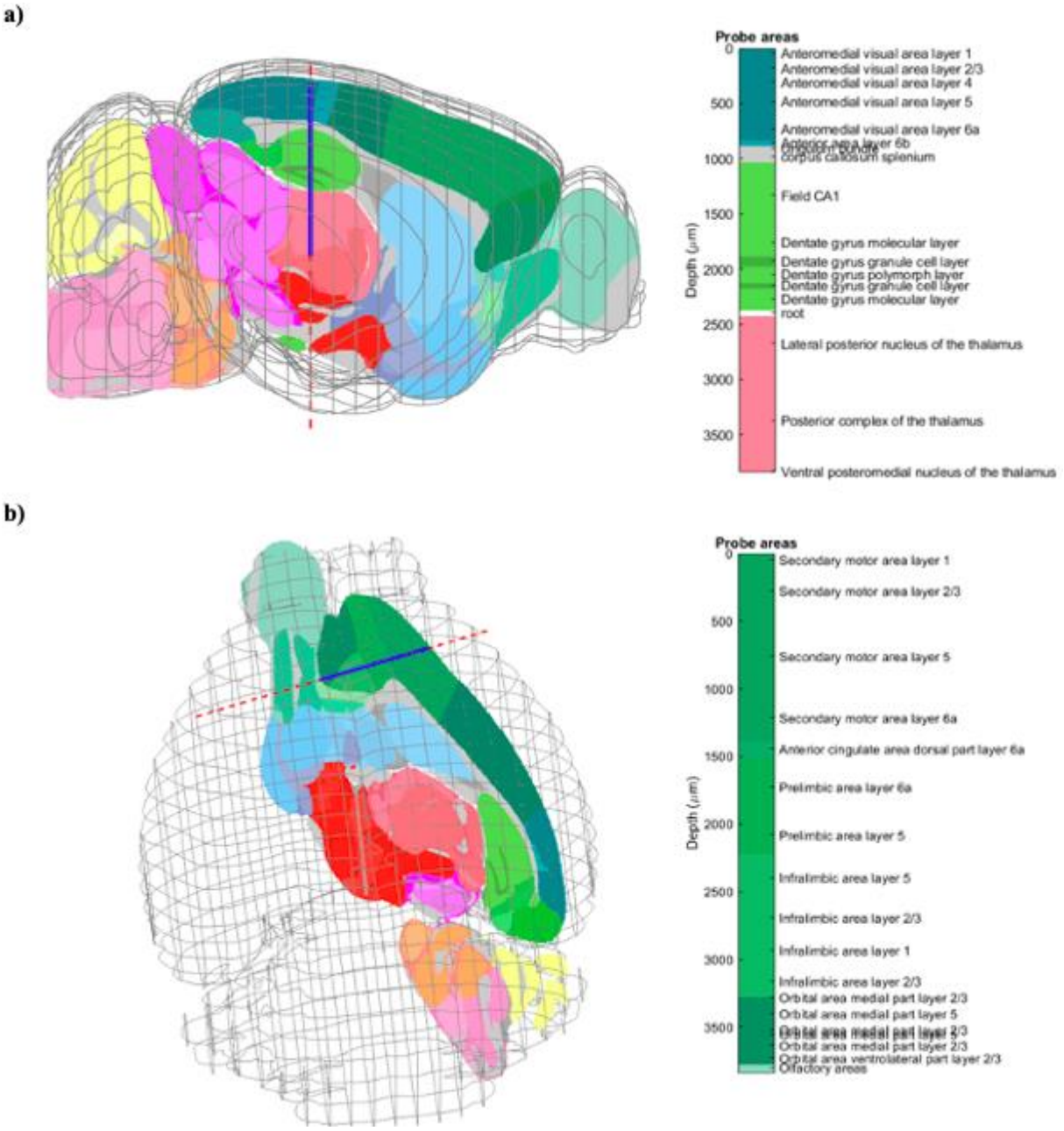

Figure 16. Trajectories of the Neuropixels probes and regions of interest. Section a) shows the trajectory and targeted brain regions of the caudal Neuropixels probe and section b) shows the trajectory and targeted brain regions of the rostral Neuropixels probe.

4.6 Data analysis

For data analysis, the collected data was preprocessed. Based on the behavioral data, resting-state periods were identified from the 30-minute recordings and from each recording session, a two-minute resting-state period was extracted. This extracted period was then downsampled from 500 Hz to 250 Hz to reduce file size and to optimize computational efficiency while keeping the essential frequencies. Additionally, a notch filter was used to account for the alternating current interference and the ECoG grids were re-referenced using a naive Laplacian method to improve the spatial resolution. To separate true brain activity from artifacts such as

muscle activity and electrical noise, an independent component analysis (ICA) was performed on the resting-state data. A Morlet wavelet filtering was used to analyze frequency-specific patterns from delta, theta, alpha, beta, and gamma frequencies. Lastly, based on a previously established mapping of recording channels connected to respective brain regions shown in figure 15 was used to link the electrophysiological data to correct anatomical regions.

With the preprocessed resting-state data, phase locking value (PLV) was calculated to analyze phase synchrony between brain regions. For temporal analysis a dynamic functional connectivity (DFC) was calculated and lastly, amplitude correlation analysis (ACA) was used to detect how the correlation of amplitude changes over time between different brain regions.

The original code for data analysis was provided by the Palva Lab and it was edited with an artificial intelligence system to create an automated analysis pipeline requiring minimal human intervention. The edited code was audited by the original code writer to check for possible errors before implementing to the analysis pipeline.

5 Acknowledgements

I would like to thank my supervisors professor Eero Castrén for making this project possible, and Raz Balin for the guidance and support during the entire thesis process. I would also like to thank all the Trophins lab members for the great company and support, especially those in the same office room. I thank the Palva labs for the assistance in the data analysis part for providing the original code and for auditing the changes made to it. Lastly, I thank all the other people close to me for the non-scientific support during this thesis process.

6 Abbreviations

ACA	Amplitude correlation analysis
ACC	Anterior cingulate cortex
aCSF	Artificial cerebrospinal fluid
BDNF	Brain derived neurotrophic factor
CEN	Central executive network
CMS	Chronic mild stress
DFC	Dynamic functional connectivity
DMN	Default mode network
ECoG	Electrocorticography
EEG	Electroencephalography
FAA	Frontal alpha asymmetry
HPA	Hypothalamus-pituitary-adrenal
IPL	Inferior parietal lobule
MDD	Major depressive disorder
MEG	Magnetoencephalography
MPFC	Medial prefrontal cortex
NGF	Nerve growth factor
NT-3	Neurotrophin-3
NT-4	Neurotrophin-4
PCC	Posterior cingulate cortex
PDMS	polymethylsiloxane
PFC	Prefrontal cortex

PLV	Phase locking value
Rsp	Retrosplenial cortex
S.C.	Subcutaneous
SN	Salience network
SNRI	Serotonin and noradrenaline reuptake inhibitor
SSRI	Selective serotonin reuptake inhibitor
Trk	Tropomyosin receptor kinase
μECOG	Micro-electrocorticography

References

Beggs, J. M. (2022). Addressing skepticism of the critical brain hypothesis. *Frontiers in Computational Neuroscience*, *16*. https://doi.org/10.3389/fncom.2022.703865

Buckner, R. L., Andrews-Hanna, J. R., & Schacter, D. L. (2008). The Brain's Default Network. *Annals of the New York Academy of Sciences*, *1124*(1), 1–38. https://doi.org/10.1196/annals.1440.011

Buckner, R. L., & DiNicola, L. M. (2019). The brain's default network: updated anatomy, physiology and evolving insights. *Nature Reviews Neuroscience*, *20*(10), 593–608. https://doi.org/10.1038/s41583-019-0212-7

Casarotto, P. C., Girych, M., Fred, S. M., Kovaleva, V., Moliner, R., Enkavi, G., Biojone, C., Cannarozzo, C., Sahu, M. P., Kaurinkoski, K., Brunello, C. A., Steinzeig, A., Winkel, F., Patil, S., Vestring, S., Serchov, T., Diniz, C. R. A. F., Laukkanen, L., Cardon, I., … Castrén, E. (2021). Antidepressant drugs act by directly binding to TRKB neurotrophin receptors. *Cell*, *184*(5), 1299-1313.e19. https://doi.org/10.1016/j.cell.2021.01.034

Castrén, E., & Antila, H. (2017). Neuronal plasticity and neurotrophic factors in drug responses. *Molecular Psychiatry*, *22*(8), 1085–1095. https://doi.org/10.1038/mp.2017.61

Cavanagh, J. F. (2019). Electrophysiology as a theoretical and methodological hub for the neural sciences. *Psychophysiology*, *56*(2). https://doi.org/10.1111/psyp.13314

Cocchi, L., Gollo, L. L., Zalesky, A., & Breakspear, M. (2017). Criticality in the brain: A synthesis of neurobiology, models and cognition. *Progress in Neurobiology*, *158*, 132–152. https://doi.org/10.1016/j.pneurobio.2017.07.002

Cui, L., Li, S., Wang, S., Wu, X., Liu, Y., Yu, W., Wang, Y., Tang, Y., Xia, M., & Li, B. (2024). Major depressive disorder: hypothesis, mechanism, prevention and treatment. *Signal Transduction and Targeted Therapy*, *9*(1), 30. https://doi.org/10.1038/s41392-024-01738-y

Destexhe, A., & Touboul, J. D. (2021). Is There Sufficient Evidence for Criticality in Cortical Systems? *Eneuro*, *8*(2), ENEURO.0551-20.2021. https://doi.org/10.1523/ENEURO.0551-20.2021

Duman, R. S., Aghajanian, G. K., Sanacora, G., & Krystal, J. H. (2016). Synaptic plasticity and depression: new insights from stress and rapid-acting antidepressants. *Nature Medicine*, *22*(3), 238–249. https://doi.org/10.1038/nm.4050

Duman, R. S., Sanacora, G., & Krystal, J. H. (2019). Altered Connectivity in Depression: GABA and Glutamate Neurotransmitter Deficits and Reversal by Novel Treatments. *Neuron*, *102*(1), 75–90. https://doi.org/10.1016/j.neuron.2019.03.013

Fernández-Palleiro, P., Rivera-Baltanás, T., Rodrigues-Amorim, D., Fernández-Gil, S., del Carmen Vallejo-Curto, M., Álvarez-Ariza, M., López, M., Rodriguez-Jamardo, C., Luis Benavente, J., de las Heras, E., Manuel Olivares, J., & Spuch, C. (2020). Brainwaves

Oscillations as a Potential Biomarker for Major Depression Disorder Risk. *Clinical EEG and Neuroscience*, *51*(1), 3–9. https://doi.org/10.1177/1550059419876807

Fuscà, M., Siebenhühner, F., Wang, S. H., Myrov, V., Arnulfo, G., Nobili, L., Palva, J. M., & Palva, S. (2023). Brain criticality predicts individual levels of inter-areal synchronization in human electrophysiological data. *Nature Communications*, *14*(1), 4736. https://doi.org/10.1038/s41467-023-40056-9

Gozzi, A., & Schwarz, A. J. (2016). Large-scale functional connectivity networks in the rodent brain. *NeuroImage*, *127*, 496–509. https://doi.org/10.1016/j.neuroimage.2015.12.017

Gozzi, A., & Zerbi, V. (2023). Modeling Brain Dysconnectivity in Rodents. *Biological Psychiatry*, *93*(5), 419–429. https://doi.org/10.1016/j.biopsych.2022.09.008

Grandjean, J., Azzinnari, D., Seuwen, A., Sigrist, H., Seifritz, E., Pryce, C. R., & Rudin, M. (2016). Chronic psychosocial stress in mice leads to changes in brain functional connectivity and metabolite levels comparable to human depression. *NeuroImage*, *142*, 544–552. https://doi.org/10.1016/j.neuroimage.2016.08.013

Hahn, G., Ponce-Alvarez, A., Deco, G., Aertsen, A., & Kumar, A. (2019). Portraits of communication in neuronal networks. *Nature Reviews Neuroscience*, *20*(2), 117–127. https://doi.org/10.1038/s41583-018-0094-0

Hamilton, J. P., Farmer, M., Fogelman, P., & Gotlib, I. H. (2015). Depressive Rumination, the Default-Mode Network, and the Dark Matter of Clinical Neuroscience. *Biological Psychiatry*, *78*(4), 224–230. https://doi.org/10.1016/j.biopsych.2015.02.020

Hamilton, J. P., Furman, D. J., Chang, C., Thomason, M. E., Dennis, E., & Gotlib, I. H. (2011). Default-Mode and Task-Positive Network Activity in Major Depressive Disorder: Implications for Adaptive and Maladaptive Rumination. *Biological Psychiatry*, *70*(4), 327–333. https://doi.org/10.1016/j.biopsych.2011.02.003

Heiney, K., Huse Ramstad, O., Fiskum, V., Christiansen, N., Sandvig, A., Nichele, S., & Sandvig, I. (2021). Criticality, Connectivity, and Neural Disorder: A Multifaceted Approach to Neural Computation. *Frontiers in Computational Neuroscience*, *15*. https://doi.org/10.3389/fncom.2021.611183

Henckens, M. J. A. G., van der Marel, K., van der Toorn, A., Pillai, A. G., Fernández, G., Dijkhuizen, R. M., & Joëls, M. (2015). Stress-induced alterations in large-scale functional networks of the rodent brain. *NeuroImage*, *105*, 312–322. https://doi.org/10.1016/j.neuroimage.2014.10.037

Herrmann, C. S., Strüber, D., Helfrich, R. F., & Engel, A. K. (2016). EEG oscillations: From correlation to causality. *International Journal of Psychophysiology*, *103*, 12–21. https://doi.org/10.1016/j.ijpsycho.2015.02.003

Hillhouse, T. M., & Porter, J. H. (2015). A brief history of the development of antidepressant drugs: From monoamines to glutamate. *Experimental and Clinical Psychopharmacology*, *23*(1), 1–21. https://doi.org/10.1037/a0038550

Hübener, M., & Bonhoeffer, T. (2014). Neuronal Plasticity: Beyond the Critical Period. *Cell*, *159*(4), 727–737. https://doi.org/10.1016/j.cell.2014.10.035

Ippolito, G., Bertaccini, R., Tarasi, L., Di Gregorio, F., Trajkovic, J., Battaglia, S., & Romei, V. (2022). The Role of Alpha Oscillations among the Main Neuropsychiatric Disorders in the Adult and Developing Human Brain: Evidence from the Last 10 Years of Research. *Biomedicines*, *10*(12), 3189. https://doi.org/10.3390/biomedicines10123189

Jun, J. J., Steinmetz, N. A., Siegle, J. H., Denman, D. J., Bauza, M., Barbarits, B., Lee, A. K., Anastassiou, C. A., Andrei, A., Aydın, Ç., Barbic, M., Blanche, T. J., Bonin, V., Couto, J., Dutta, B., Gratiy, S. L., Gutnisky, D. A., Häusser, M., Karsh, B., … Harris, T. D. (2017). Fully integrated silicon probes for high-density recording of neural activity. *Nature*, *551*(7679), 232–236. https://doi.org/10.1038/nature24636

Kaiser, R. H., Andrews-Hanna, J. R., Wager, T. D., & Pizzagalli, D. A. (2015). Large-Scale Network Dysfunction in Major Depressive Disorder. *JAMA Psychiatry*, *72*(6), 603. https://doi.org/10.1001/jamapsychiatry.2015.0071

Kane, J., Cavanagh, J. F., & Dillon, D. G. (2019). Reduced Theta Power During Memory Retrieval in Depressed Adults. *Biological Psychiatry: Cognitive Neuroscience and Neuroimaging*, *4*(7), 636–643. https://doi.org/10.1016/j.bpsc.2019.03.004

Lee, J. Y., Park, S. H., Kim, Y., Cho, Y. U., Park, J., Hong, J.-H., Kim, K., Shin, J., Ju, J. E., Min, I. S., Sang, M., Shin, H., Jeong, U.-J., Gao, Y., Li, B., Zhumbayeva, A., Kim, K. Y., Hong, E.-B., Nam, M.-H., … Yu, K. J. (2022). Foldable three dimensional neural electrode arrays for simultaneous brain interfacing of cortical surface and intracortical multilayers. *Npj Flexible Electronics*, *6*(1), 86. https://doi.org/10.1038/s41528-022-00219-y

Lu, H., Zou, Q., Gu, H., Raichle, M. E., Stein, E. A., & Yang, Y. (2012). Rat brains also have a default mode network. *Proceedings of the National Academy of Sciences*, *109*(10), 3979–3984. https://doi.org/10.1073/pnas.1200506109

Malhi, G. S., & Mann, J. J. (2018). Depression. *The Lancet*, *392*(10161), 2299–2312. https://doi.org/10.1016/S0140-6736(18)31948-2

Marchetti, I., Koster, E. H. W., Sonuga-Barke, E. J., & De Raedt, R. (2012). The Default Mode Network and Recurrent Depression: A Neurobiological Model of Cognitive Risk Factors. *Neuropsychology Review*, *22*(3), 229–251. https://doi.org/10.1007/s11065-012-9199-9

Mercier, M. R., Dubarry, A.-S., Tadel, F., Avanzini, P., Axmacher, N., Cellier, D., Vecchio, M. Del, Hamilton, L. S., Hermes, D., Kahana, M. J., Knight, R. T., Llorens, A., Megevand, P., Melloni, L., Miller, K. J., Piai, V., Puce, A., Ramsey, N. F., Schwiedrzik, C. M., … Oostenveld, R. (2022). Advances in human intracranial electroencephalography research,

guidelines and good practices. *NeuroImage*, *260*, 119438. https://doi.org/10.1016/j.neuroimage.2022.119438

Mohammadi, Z., Denman, D. J., Klug, A., & Lei, T. C. (2024). A fully automatic multichannel neural spike sorting algorithm with spike reduction and positional feature. *Journal of Neural Engineering*, *21*(4), 046039. https://doi.org/10.1088/1741-2552/ad647d

Moliner, R., Girych, M., Brunello, C. A., Kovaleva, V., Biojone, C., Enkavi, G., Antenucci, L., Kot, E. F., Goncharuk, S. A., Kaurinkoski, K., Kuutti, M., Fred, S. M., Elsilä, L. V., Sakson, S., Cannarozzo, C., Diniz, C. R. A. F., Seiffert, N., Rubiolo, A., Haapaniemi, H., … Castrén, E. (2023). Psychedelics promote plasticity by directly binding to BDNF receptor TrkB. *Nature Neuroscience*, *26*(6), 1032–1041. https://doi.org/10.1038/s41593-023-01316-5

Mulders, P. C., van Eijndhoven, P. F., Schene, A. H., Beckmann, C. F., & Tendolkar, I. (2015). Resting-state functional connectivity in major depressive disorder: A review. *Neuroscience & Biobehavioral Reviews*, *56*, 330–344. https://doi.org/10.1016/j.neubiorev.2015.07.014

Murray, F., Smith, D. W., & Hutson, P. H. (2008). Chronic low dose corticosterone exposure decreased hippocampal cell proliferation, volume and induced anxiety and depression like behaviours in mice. *European Journal of Pharmacology*, *583*(1), 115–127. https://doi.org/10.1016/j.ejphar.2008.01.014

O'Byrne, J., & Jerbi, K. (2022). How critical is brain criticality? *Trends in Neurosciences*, *45*(11), 820–837. https://doi.org/10.1016/j.tins.2022.08.007

Palva, S., & Palva, J. M. (2018). Roles of Brain Criticality and Multiscale Oscillations in Temporal Predictions for Sensorimotor Processing. *Trends in Neurosciences*, *41*(10), 729–743. https://doi.org/10.1016/j.tins.2018.08.008

Planchez, B., Surget, A., & Belzung, C. (2019). Animal models of major depression: drawbacks and challenges. *Journal of Neural Transmission*, *126*(11), 1383–1408. https://doi.org/10.1007/s00702-019-02084-y

Power, J. D., & Schlaggar, B. L. (2017). Neural plasticity across the lifespan. *WIREs Developmental Biology*, *6*(1). https://doi.org/10.1002/wdev.216

Raichle, M. E., MacLeod, A. M., Snyder, A. Z., Powers, W. J., Gusnard, D. A., & Shulman, G. L. (2001). A default mode of brain function. *Proceedings of the National Academy of Sciences*, *98*(2), 676–682. https://doi.org/10.1073/pnas.98.2.676

Samuels, B. A., Leonardo, E. D., Gadient, R., Williams, A., Zhou, J., David, D. J., Gardier, A. M., Wong, E. H. F., & Hen, R. (2011). Modeling treatment-resistant depression. *Neuropharmacology*, *61*(3), 408–413. https://doi.org/10.1016/j.neuropharm.2011.02.017

Shokoueinejad, M., Park, D.-W., Jung, Y. H., Brodnick, S. K., Novello, J., Dingle, A., Swanson, K. I., Baek, D.-H., Suminski, A. J., Lake, W. B., Ma, Z., & Williams, J. (2019). Progress in

the Field of Micro-Electrocorticography. *Micromachines*, *10*(1), 62. https://doi.org/10.3390/mi10010062

Shulman, G. L., Fiez, J. A., Corbetta, M., Buckner, R. L., Miezin, F. M., Raichle, M. E., & Petersen, S. E. (1997). Common Blood Flow Changes across Visual Tasks: II. Decreases in Cerebral Cortex. *Journal of Cognitive Neuroscience*, *9*(5), 648–663. https://doi.org/10.1162/jocn.1997.9.5.648

Sihn, D., Kim, J. S., Kwon, O.-S., & Kim, S.-P. (2023). Breakdown of long-range spatial correlations of infraslow amplitude fluctuations of EEG oscillations in patients with current and past major depressive disorder. *Frontiers in Psychiatry*, *14*. https://doi.org/10.3389/fpsyt.2023.1132996

Smallwood, J., Bernhardt, B. C., Leech, R., Bzdok, D., Jefferies, E., & Margulies, D. S. (2021). The default mode network in cognition: a topographical perspective. *Nature Reviews Neuroscience*, *22*(8), 503–513. https://doi.org/10.1038/s41583-021-00474-4

Song, J., & Kim, Y. (2021). Animal models for the study of depressive disorder. *CNS Neuroscience & Therapeutics*, *27*(6), 633–642. https://doi.org/10.1111/cns.13622

Stafford, J. M., Jarrett, B. R., Miranda-Dominguez, O., Mills, B. D., Cain, N., Mihalas, S., Lahvis, G. P., Lattal, K. M., Mitchell, S. H., David, S. V., Fryer, J. D., Nigg, J. T., & Fair, D. A. (2014). Large-scale topology and the default mode network in the mouse connectome. *Proceedings of the National Academy of Sciences*, *111*(52), 18745–18750. https://doi.org/10.1073/pnas.1404346111

Steinmetz, N. A., Koch, C., Harris, K. D., & Carandini, M. (2018). Challenges and opportunities for large-scale electrophysiology with Neuropixels probes. *Current Opinion in Neurobiology*, *50*, 92–100. https://doi.org/10.1016/j.conb.2018.01.009

Takahashi, A., Chung, J.-R., Zhang, S., Zhang, H., Grossman, Y., Aleyasin, H., Flanigan, M. E., Pfau, M. L., Menard, C., Dumitriu, D., Hodes, G. E., McEwen, B. S., Nestler, E. J., Han, M.-H., & Russo, S. J. (2017). Establishment of a repeated social defeat stress model in female mice. *Scientific Reports*, *7*(1), 12838. https://doi.org/10.1038/s41598-017-12811-8

Thut, G., Miniussi, C., & Gross, J. (2012). The Functional Importance of Rhythmic Activity in the Brain. *Current Biology*, *22*(16), R658–R663. https://doi.org/10.1016/j.cub.2012.06.061

von Bernhardi, R., Bernhardi, L. E., & Eugenín, J. (2017). *What Is Neural Plasticity?* (pp. 1–15). https://doi.org/10.1007/978-3-319-62817-2_1

Wang, X.-J. (2010). Neurophysiological and Computational Principles of Cortical Rhythms in Cognition. *Physiological Reviews*, *90*(3), 1195–1268. https://doi.org/10.1152/physrev.00035.2008

Whitesell, J. D., Liska, A., Coletta, L., Hirokawa, K. E., Bohn, P., Williford, A., Groblewski, P. A., Graddis, N., Kuan, L., Knox, J. E., Ho, A., Wakeman, W., Nicovich, P. R., Nguyen, T. N., van Velthoven, C. T. J., Garren, E., Fong, O., Naeemi, M., Henry, A. M., … Harris, J.

A. (2021). Regional, Layer, and Cell-Type-Specific Connectivity of the Mouse Default Mode Network. *Neuron*, *109*(3), 545-559.e8. https://doi.org/10.1016/j.neuron.2020.11.011

Wise, T., Marwood, L., Perkins, A. M., Herane-Vives, A., Joules, R., Lythgoe, D. J., Luh, W.-M., Williams, S. C. R., Young, A. H., Cleare, A. J., & Arnone, D. (2017). Instability of default mode network connectivity in major depression: a two-sample confirmation study. *Translational Psychiatry*, *7*(4), e1105–e1105. https://doi.org/10.1038/tp.2017.40

Yan, C.-G., Chen, X., Li, L., Castellanos, F. X., Bai, T.-J., Bo, Q.-J., Cao, J., Chen, G.-M., Chen, N.-X., Chen, W., Cheng, C., Cheng, Y.-Q., Cui, X.-L., Duan, J., Fang, Y.-R., Gong, Q.-Y., Guo, W.-B., Hou, Z.-H., Hu, L., … Zang, Y.-F. (2019). Reduced default mode network functional connectivity in patients with recurrent major depressive disorder. *Proceedings of the National Academy of Sciences*, *116*(18), 9078–9083. https://doi.org/10.1073/pnas.1900390116

Zhu, X., Zhu, Q., Shen, H., Liao, W., & Yuan, F. (2017). Rumination and Default Mode Network Subsystems Connectivity in First-episode, Drug-Naive Young Patients with Major Depressive Disorder. *Scientific Reports*, *7*(1), 43105. https://doi.org/10.1038/srep43105

Zimmern, V. (2020). Why Brain Criticality Is Clinically Relevant: A Scoping Review. *Frontiers in Neural Circuits*, *14*. https://doi.org/10.3389/fncir.2020.00054

Appendices

Appendix 1 Caudal intracranial phase locking values of delta, beta, and gamma frequencies

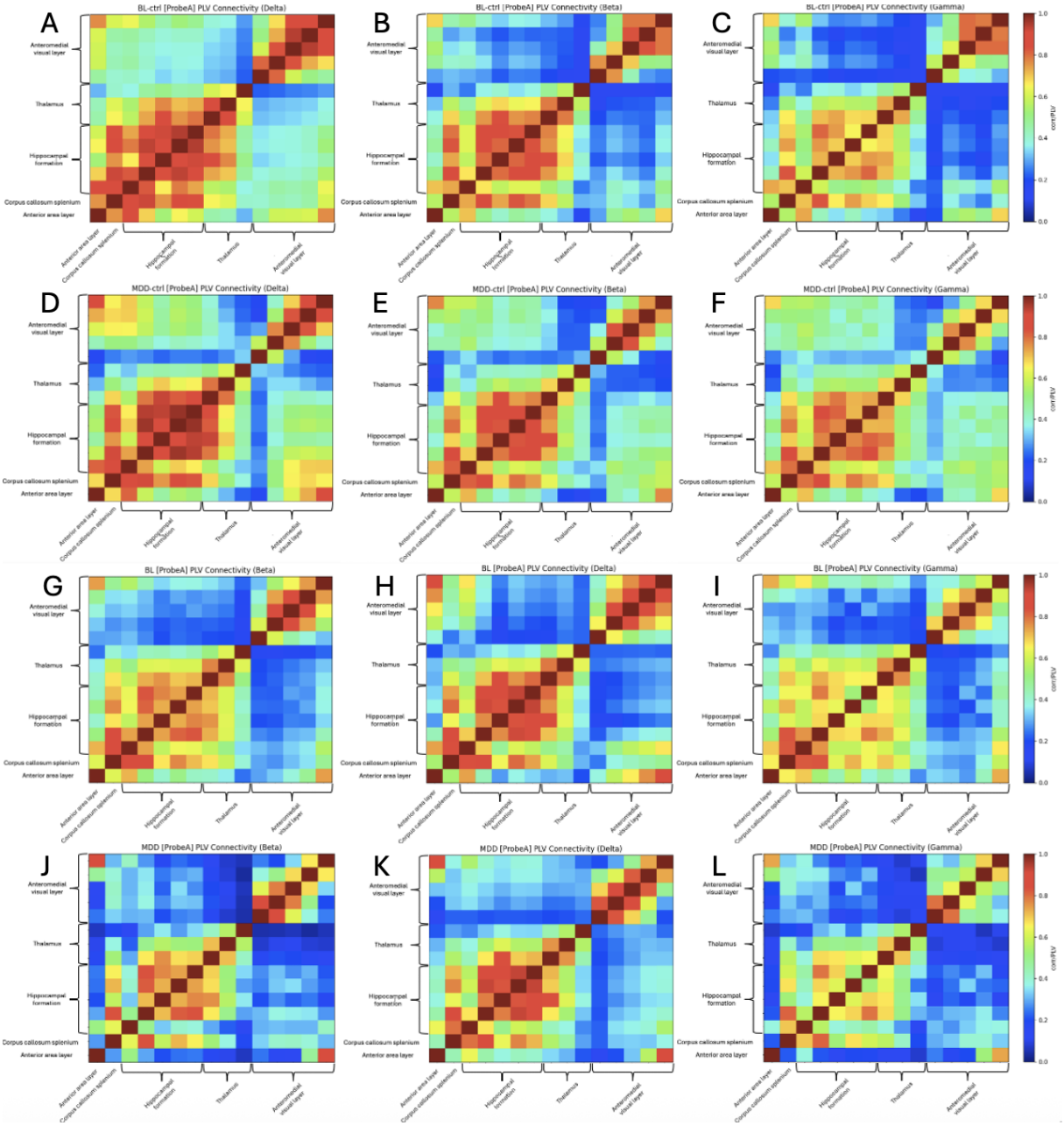

Figure A1. Phase locking values of delta, beta, and gamma frequencies from caudal intracranial electrode. In sections A-F are the control group's values with A-C being the baseline and D-F being the post-21-days values. A and D represent delta, B and E represent beta, and C and F represent gamma. In sections G-L are the treatment group's values with G-I being the baseline and J-L being the post-21-days values. G and J represent delta, H and K represent beta, and I and L represent gamma.

Appendix 2 Rostral intracranial phase locking values of delta, beta, and gamma frequencies

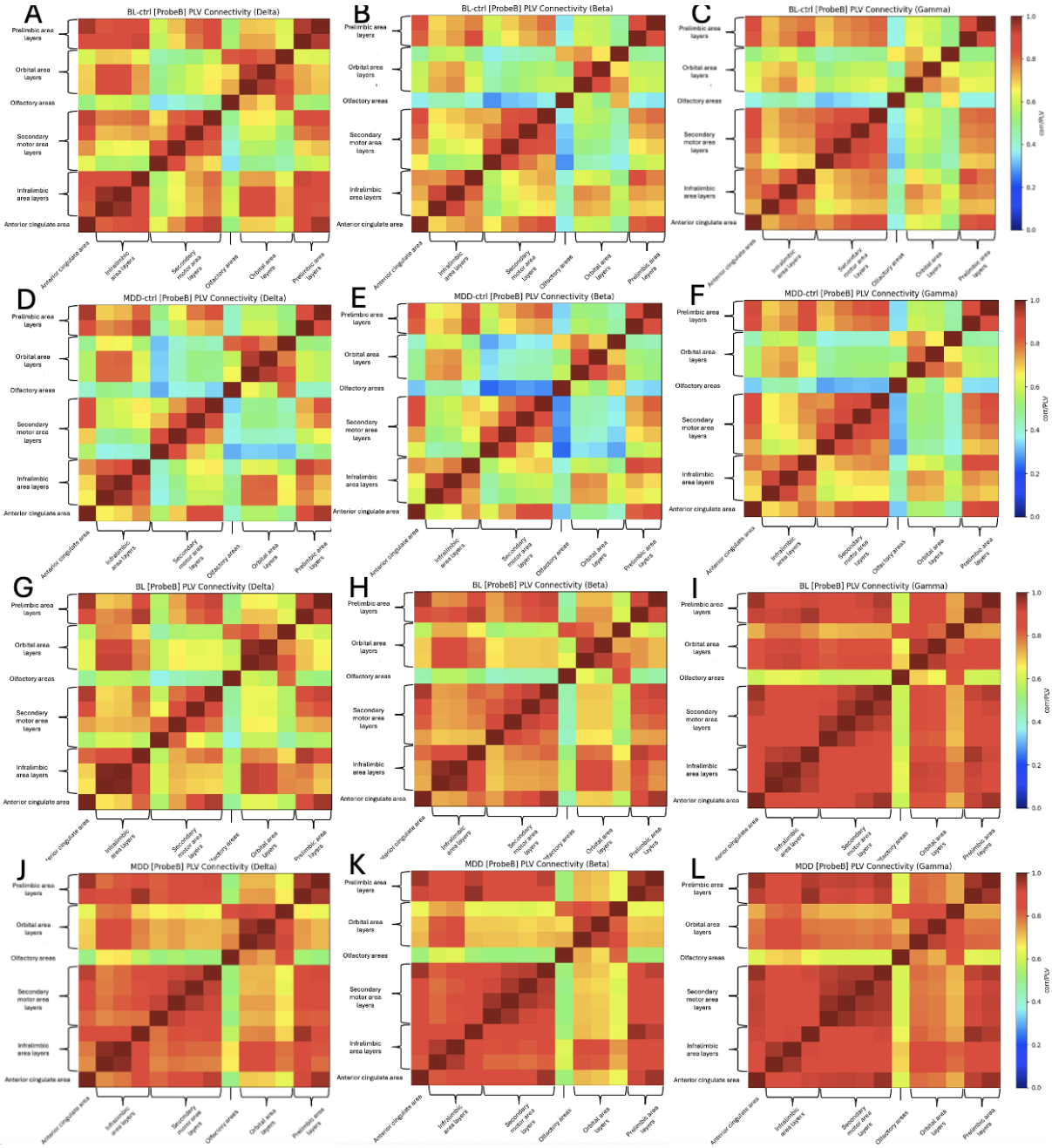

Figure A2. Phase locking values of delta, beta, and gamma frequencies from rostral intracranial electrode. In sections A-F are the control group's values with A-C being the baseline and D-F being the post-21-days values. A and D represent delta, B and E represent beta, and C and F represent gamma. In sections G-L are the treatment group's values with G-I being the baseline and J-L being the post-21-days values. G and J represent delta, H and K represent beta, and I and L represent gamma.

Appendix 3 Cortical phase locking values of delta, beta, and gamma frequencies

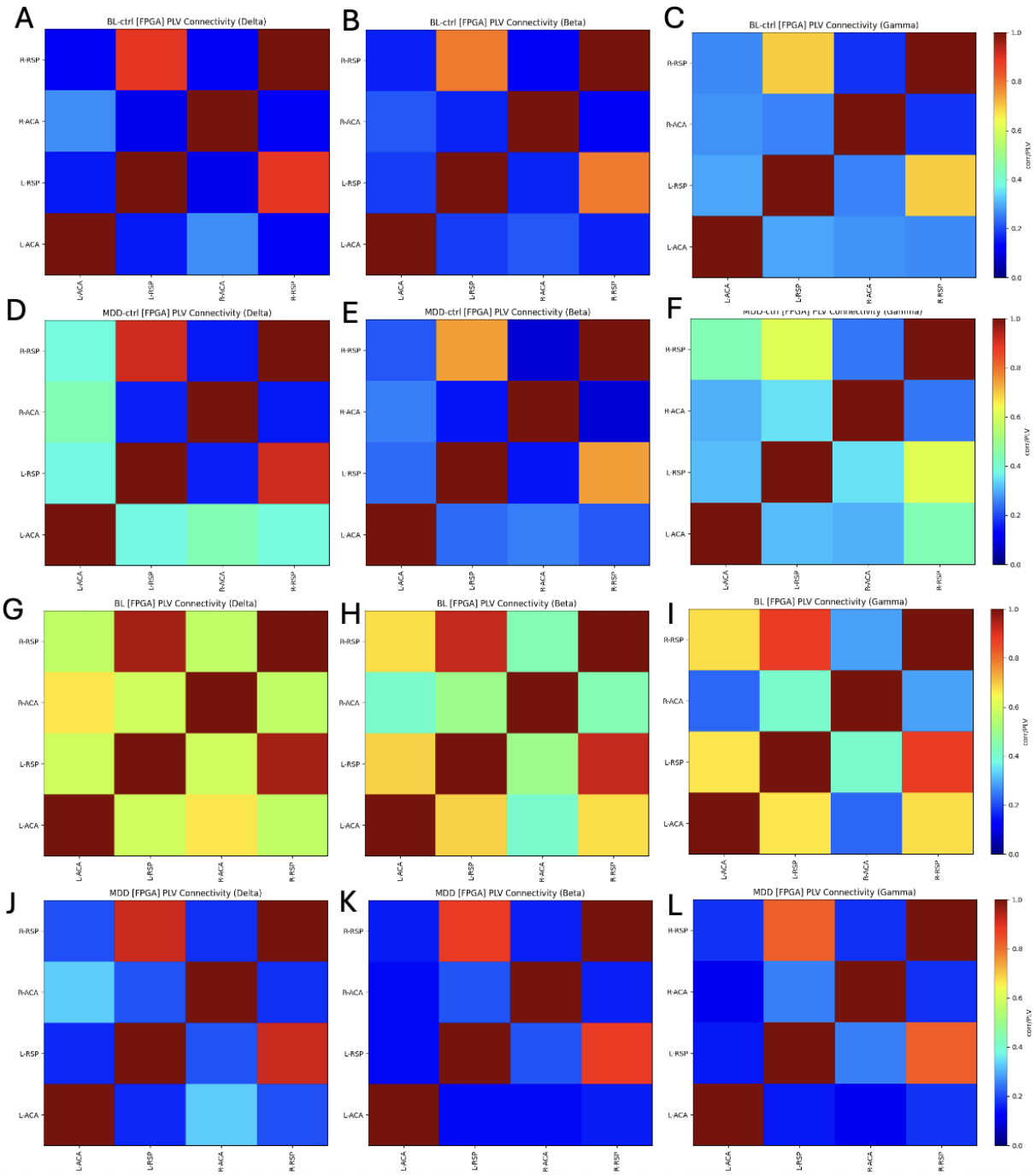

Figure A3. Phase locking values of delta, beta, and gamma frequencies from cortical micro-electrocorticography grids. In sections A-F are the control group's values with A-C being the baseline and D-F being the post-21-days values. A and D represent delta, B and E represent beta, and C and F represent gamma. In sections G-L are the treatment group's values with G-I being the baseline and J-L being the post-21-days values. G and J represent delta, H and K represent beta, and I and L represent gamma.